An Analysis of Porphyrin Molecular Flexibility—Use of Porphyrin Diacids

Beisong Cheng,[†] Orde Q. Munro,[†,§] Helder M. Marques,[⊥] and W. Robert Scheidt*[,†]

Contribution from the Department of Chemistry and Biochemistry, University of Notre Dame, Notre Dame, Indiana 46556, and Centre for Molecular Design, Department of Chemistry, University of the Witwatersrand, Wits 2050, Johannesburg, South Africa

Received May 19, 1997[⊗]

Abstract: The crystal structures of three porphyrin diacid species, $[H_4OEP](ClO_4)_2$, $[H_4TPP](ClO_4)_2$, and $[H_4TMP](ClO_4)_2$, have been determined from low-temperature X-ray diffraction data to delineate how the peripheral substituents of the porphyrin affect the overall *molecular flexibility*. $[H_4OEP](ClO_4)_2$ ($|C_b| = 0.46$ Å), $[H_4TMP](ClO_4)_2$ ($|C_b| = 0.67$ Å, molecule **1**), and $[H_4TPP](ClO_4)_2$ ($|C_b| = 0.93$ Å) show increasingly saddled core conformations with effective D_{2d} symmetry. The mean porphyrin−aryl group dihedral angles in $[H_4TPP](ClO_4)_2$ and $[H_4TMP](ClO_4)_2$ (molecule **1**) are 27(2)° and 63(13)°, respectively. The steric bulk of the mesityl substituents in $[H_4TMP]^{2+}$ limits the range of observed porphyrin−aryl group dihedral angles to >50° and, consequently, the magnitude of the core distortion. $[H_4TMP]^{2+}$ is therefore less flexible than $[H_4TPP]^{2+}$. Molecular mechanics calculations, using a modified version of MM2(87) and a newly developed force field for porphyrin diacids, correctly predict that the flexibility of *meso*-tetraaryl porphyrin diacids decreases as the steric bulk of the peripheral substituents increases: $[H_4TPyP]^{2+} \approx [H_4TPP]^{2+} > [H_4T\text{-}2,6\text{-}(OH)_2\ PP]^{2+} \approx [H_4T\text{-}2,6\text{-}F_2\ PP]^{2+} > [H_4T\text{-}2,6\text{-}Cl_2\ PP]^{2+} \approx [H_4TMP]^{2+}$. Grid searches of conformational space for $[H_4porphine]^{2+}$, $[H_4OEP]^{2+}$, $[H_4TPP]^{2+}$, and $[H_4T\text{-}2,6\text{-}Cl_2\ PP]^{2+}$ located pairs of inversion-related minima with D_{2d} -saddled and C_{2h}-stepped core conformations. The *in vacuo* strain energy barrier to inversion of the lowest-energy D_{2d}-saddled conformation increases from 0.45 kcal/mol in $[H_4porphine]^{2+}$ to 1.9 kcal/mol in $[H_4T\text{-}2,6\text{-}Cl_2PP]^{2+}$. The calculations indicate that the relative stability and magnitude of distortion of the D_{2d} isomer increases as the steric bulk of the peripheral substituents increases; $[H_4OEP]^{2+}$ is therefore calculated to be less distorted than $[H_4TPP]^{2+}$, in agreement with the X-ray structures of these species.

Introduction

Diverse biological systems, ranging from vertebrates to algae and bacteria, utilize porphyrins or other tetrapyrrole-based macrocycles[1−6] as prosthetic groups or coenzymes. The biological functions of these cofactors are thought to depend on intricate control mechanisms imposed on the intrinsic reactivity of the metal ion and/or tetrapyrrole macrocycle by the protein. An example is the photosynthetic reaction center from the purple bacterium *Rhodopseudomonas viridis*.[7] The X-ray structure of this membrane-bound protein reveals that the two π-stacked bacteriochlorophyll-*b* molecules of the special pair exhibit measurably different degrees of distortion.[8] Deisenhofer and Michel[8] have suggested that this conformational difference may lead to unequal charge distribution between the chlorin groups and, consequently, unidirectional electron transfer down the sequence of tetrapyrrole cofactors contained within the L subunit, rather than along those of both L and M subunits. This is consistent with spectroscopic studies and MO calculations which have shown that significant changes in the electronic properties of chlorins and porphyrins attend changes in the extent of macrocycle distortion.[3a,9]

That the conformation of a porphyrin may play a decisive role in controlling the functioning of a protein raises several fundamental questions. What determines the overall *molecular flexibility* of porphyrins and other tetrapyrrole macrocycles? Does porphyrin ring flexibility depend on the substitution pattern of the macrocycle? If so, are peripheral substituents required to engender a particular type of conformational distortion? These questions are particularly relevant in the case of hemoproteins since there is evidence to support the idea that some bis-histidine multiheme cytochromes, for example, cytochrome c_3 form *Desulfovibrio vulgaris*,[10] are able to fine-tune the redox potential[11] and electronic properties[12] of each heme group by maintaining unique axial ligand orientations, and thus porphyrin

* To whom correspondence should be addressed. E-mail: Scheidt.1@nd.edu.

† University of Notre Dame.

§ Present address: Department of Chemistry, University of Natal, Private Bag X01, Pietermaritzburg 3209, South Africa.

⊥ University of the Witwatersrand.

⊗ Abstract published in *Advance ACS Abstracts,* October 15, 1997.

(1) *Porphyrins and Metalloporphyrins*; Smith, K. M., Ed.; Elsevier/North-Holland Inc.: New York, 1976.

(2) *The Porphyrins*; Dolphin, D., Ed.; Academic: New York, 1978; Vols. 1−7.

(3) (a) Barkigia, K. M.; Chantranupong, L.; Smith, K. M.; Fajer, J. *J. Am. Chem. Soc.* **1988**, *110*, 7566. (b) Strauss, S. H.; Silver, M. E.; Ibers, J. A. *J. Am. Chem. Soc.* **1983**, *105*, 4108. (c) Chow, H.-C.; Serlin, R.; Strouse, C. E. *J. Am. Chem. Soc.* **1975**, *97*, 7230; **1975**, *97*, 7237. (d) Gallucci, J. C.; Swepston, P. N.; Ibers, J. A. *Acta Crystallogr., Sect. B* **1982**, *B38*, 2134.

(4) (a) Murphy, M. J.; Siegel, L. M.; Kamin, H.; Rosenthal, D. *J. Biol. Chem.* **1973**, *248*, 2801. (b) Kratky, C.; Angst, C.; Johansen, J. E. *Angew. Chem., Int. Ed. Engl.* **1981**, *20*, 211. (c) Kratky, C.; Waditschatka, R.; Angst, C.; Johansen, J. E.; Plaquevent, J. C.; Schreiber, J.; Eschenmoser, A. *Helv. Chim. Acta* **1985**, *68*, 1312.

(5) (a) B_{12}; Dolphin, D., Ed.; Wiley: New York, 1982; Vols. 1 and 2. (b) Stadtman, T. C. *Science* **1971**, *171*, 859.

(6) (a) Ellefson, W. L.; Whitman, W. B.; Wolfe, R. S. *Proc. Natl. Acad. Sci. U.S.A.* **1982**, *79*, 3707. (b) Pfaltz, A.; Livingston, D. A.; Jaun, B.; Diekert, G.; Thauer, R. K.; Eschenmoser, A. *Helv. Chim. Acta* **1985**, *68*, 1338. (c) Johansen, J. E.; Piermattie, V.; Angst, C.; Diener, E.; Kratky, C.; Eschenmoser, A. *Angew. Chem., Int. Ed. Engl.* **1981**, *20*, 261.

(7) (a) Deisenhofer, J.; Epp, O.; Miki, K.; Huber, R.; Michel, H. *J. Mol. Biol.* **1984**, *180*, 385. (b) Deisenhofer, J.; Epp, O.; Miki, K.; Huber, R.; Michel, H. *Nature* **1985**, *318*, 618.

(8) Deisenhofer, J.; Michel, H. *EMBO J.* **1989**, *8*, 2149.

(9) (a) Gudowska-Nowak, E.; Newton, M. D.; Fajer, J. *J. Phys. Chem.* **1990**, *94*, 5795. (b) Renner, M. W.; Cheng, R.-J.; Chang, C. K.; Fajer, J. *J. Phys. Chem.* **1990**, *94*, 8508.

(10) Higuchi, Y; Kusanoki, M; Matsuura, Y.; Yasuoka, N.; Kakudo, M. *J. Mol. Biol.* **1984**, *172*, 109.

S0002-7863(97)01621-1 CCC: $14.00

core conformations, at each heme center. Since it is experimentally difficult to examine the effect of peripheral substitution on the conformational flexibility of porphyrins in intact proteins, studies on suitably chosen model systems constitute an alternative for systematic evaluation of the factors that may control porphyrin ring flexibility. While it is well-known that peripherally crowded porphyrins adopt highly saddled core conformations (D_{2d} symmetry) in solution and in the solid state,[13−15] the degree of distortion in these compounds remains large and essentially fixed. Indeed, derivatives of H_2OEP[16] and H_2TPP display a wider range of core conformations than the more highly distorted D_{2d}-saddled species derived from H_2DDPP[14] or H_2OETPP.[15] For H_2OEP and H_2TPP, the conformations depend on a number of factors, e.g., the identity of the metal ion, its oxidation state, the steric bulk of the axial ligands, and the packing environment.[17,18] Moreover, when analogous derivatives of H_2OEP and H_2TPP have both been structurally characterized, it is observed that the H_2OEP derivatives are always more planar,[19] suggesting intrinsic differences in molecular flexibility that result from the substituents. Thus derivatives of porphine, H_2OEP, and H_2TPP should be the most suitable for investigating how the peripheral substitution pattern of the macrocycle affects the flexibility of the *entire* porphyrin ligand.

The central question is how to dissect the contribution made by the peripheral groups to the flexibility of the porphyrin core. Our experimental approach is to provide a constant structural perturbation to porphyrin derivatives with differing peripheral substituents and to examine the structural differences; this should provide insight into the effects that the substituent groups have on the flexibility of the porphyrin core. Specifically, our approach is based on protonating the porphyrin free bases, H_2Porph. It is known that the two unsubstituted nitrogens can be alkylated or protonated to afford mono- or dicationic derivatives with moderately to strongly distorted core conformations.[20−22] In 1968, Stone and Fleischer[20b] reported the first X-ray study on porphyrin diacid derivatives, $[H_4Porph]^{2+}$. From the observed D_{2d}-saddled conformations of $[H_4TPP]^{2+}$ and $[H_4TPyP]^{2+}$, the authors concluded that alleviating the steric strain from the protonated porphyrin nitrogens involves canting the pyrrole NH groups alternately above and below the porphyrin mean plane. Thus, from an experimental standpoint, protonating the four porphyrin nitrogens does appear to be an effective way to apply a near-constant deformation stress to the porphyrin macrocycle, and it should be possible to determine the effect that the substituent groups have on the flexibility of the porphyrin as a whole.

In 1964, Hoard suggested that the S_4-ruffled tetragonal form of H_2TPP should have a low barrier to inversion since it is relatively easily distorted from planarity in the solid state.[23] More recently, Medforth et al. measured the free energies of activation (ΔG^*) for conformational inversion in $[H_4TMTCPP]^{2+}$, $[H_4TETCPP]^{2+}$, and $[H_4TPTCPP]^{2+}$ and found that the barrier increased slightly with the length of the alkyl chain appended to the *meso*-carbons.[14] If the flexibility of a porphyrin is reduced by peripheral steric strain, as implied by the NMR data, and can be gauged from the height of the barrier to inversion, then one has available a simple method for determining the intrinsic flexibility of the system. However, although dynamic NMR methods may be used to measure the barrier to inversion in porphyrin diacids, the method fails in systems with no diastereotopic protons or intrinsically low inversion barriers.[24] Analysis of the conformational space available to a particular system using computational methods,[25] on the other hand, can provide information on the relative stabilities of isomeric structures on the potential surface, the heights of the barriers separating stable pairs of conformations, and the lowest energy pathways for conformational interconversion.

In this study we have used low-temperature X-ray crystallography to characterize the structures of three porphyrin diacid species, $[H_4OEP]^{2+}$, $[H_4TPP]^{2+}$, and $[H_4TMP]^{2+}$, as their perchlorate salts to evaluate whether changing the peripheral

(11) (a) Benosman, H.; Asso, M.; Bertrand, P.; Yagi, T.; Gayda, J.-P. *Eur. J. Biochem.* **1989**, *182*, 51. (b) Gayda, J.-P.; Benosman, H.; Bertrand, P.; More, C.; Asso, M. *Eur. J. Biochem.* **1988**, *177*, 199. (c) Gayda, J.-P.; Bertrand, P.; More, C.; Guerlesquin, F.; Bruschi, M. *Biochim. Biophys. Acta* **1985**, *829*, 262.

(12) (a) Palmer, G. *Biochem. Soc. Trans.* **1985**, *13*, 548. (b) Moura, I.; Teixeira, M.; LeGall, J.; Moura, J. J. G.; Huynh, B. H. *Eur. J. Biochem.* **1988**, *176*, 365.

(13) Barkigia, K. M.; Berber, M. D.; Fajer, J.; Medforth, C. J.; Renner, M. W.; Smith, K. M. *J. Am. Chem. Soc.* **1990**, *112*, 8851.

(14) (a) Medforth, C. J.; Senge, M. O.; Smith, K. M.; Sparks, L. D.; Shelnutt, J. A. *J. Am. Chem. Soc.* **1992**, *114*, 9859. (b) Medforth, C. J.; Senge, M. O.; Smith, K. M.; Sparks, L. D.; Shelnutt, J. A. *J. Am. Chem. Soc.* **1992**, *114*, 9859.

(15) Sparks, L. D.; Medforth, C. J.; Park, M.-S.; Chamberlain, J. R.; Ondrias, M. R.; Senge, M. O.; Smith, K. M.; Shelnutt, J. A. *J. Am. Chem. Soc.* **1993**, *115*, 581.

(16) Abbreviations: $|C_a|$, $|C_b|$, $|C_m|$, $|C_{20}|$, $|C_{20}N_4|$, and $|N_4|$, average absolute perpendicular displacements of the α-, *β*-, *meso*-carbons, porphyrin carbons, 24 atoms, and pyrrole nitrogens from the 24-atom mean porphyrin core, respectively; C_a, C_b, and C_m, porphyrin α-, *β*-, and *meso*-carbons, respectively; C_p, *meso*-aryl group carbon; H_2DDPP, 2,3,5,7,8,10,12,13,15,-17,18,20-dodecaphenylporphyrin; H_2OBrTMP, 2,3,7,8,12,13,17,18-octabromo-5,10,15,20-tetramesitylporphyrin; H_2OClTMP, 2,3,7,8,12,13,17,18-octachloro-5,10,15,20-tetramesitylporphyrin; H_2OEP, 2,3,7,8,12,13,17,18-octaethylporphyrin; H_2OETPP, 2,3,7,8,12,13,17,18-octaethyl-5,10,15,20-tetraphenylporphyrin; $[H_4Porph]^{2+}$, diacid of a porphyrin in general; H_2Porph, porphyrin in general; $[H_4porphine]^{2+}$, diacid of porphine; H_2OBrTPP, 2,3,7,8,12,13,17,18-octabromo-5,10,15,20-tetraphenylporphyrin; H_2TMP, 5,-10,15,20-tetramesitylporphyrin; H_2TPP, 5,10,15,20-tetraphenylporphyrin; H_2-TPyP, 5,10,15,20-tetrapyridylporphyrin; H_2T-2,6-Cl_2PP, 5,10,15,20-tetra-2,6-dichlorophenylporphyrin; H_2T-2,6-F_2PP, 5,10,15,20-tetra-2,6-difluorophenylporphyrin; H_2T-2,6-$(OH)_2$PP, 5,10,15,20-tetra-2,6-dihydroxyphenylporphyrin; H_2TCHP, tetracyclohexa[*b*,*g*,*l*]porphyrin; H_2TMTEP, 2,3,12,-13-tetramethyl-7,8,17,18-tetraethylporphyrin; H_2TETCPP, 5,10,15,20-tetraethyl-2,3,7,8,12,13,17,18-tetracyclopropanoporphyrin; H_2TMTCPP, 5,-10,15,20-tetramethyl-2,3,7,8,12,13,17,18-tetracyclopropanoporphyrin; H_4TPTCPP, 5,10,15,20-tetrapentyl-2,3,7,8,12,13,17,18-tetracyclopropanoporphyrin; TFA, trifluoroacetate.

(17) Scheidt, W. R.; Lee, Y. J. *Struct. Bonding* **1987**, *64*, 1.

(18) (a) Fleischer, E. B.; Miller, C. K.; Webb, L. E. *J. Am. Chem. Soc.* **1964**, *86*, 2342. (b) Scheidt, W. R.; Mondal, J. U.; Eigenbrot, C. W.; Adler, A.; Radonovich, L. J.; Hoard, J. L. *Inorg. Chem.* **1986**, *25*, 795.

(19) Scheidt, W. R.; Turowska-Tyrk, I. *Inorg. Chem.* **1994**, *33*, 1314.

(20) Tetrapyrrole diacid species: (a) Sheldrick, W. S. *J. Chem. Soc., Perkin Trans. 2* **1976**, 453. (b) Stone, A.; Fleischer, E. B. *J. Am. Chem. Soc.* **1968**, *90*, 2735. (c) Cetinkaya, E.; Johnson, A. W.; Lappert, M. F.; McLaughlin, G. M.; Muir, K. W. *J. Chem. Soc., Dalton Trans.* **1974**, 1237. (d) Senge, M. O.; Forsyth, T. P.; Nguyen, L. T.; Smith, K. M. *Angew. Chem., Int. Ed. Engl.* **1994**, *33*, 2485. (e) Navaza, A.; deRango, C.; Charpin, P. *Acta Crystallogr., Sect. C* **1983**, *C39*, 1625. (f) Nguyen, L. T.; Senge, M. O.; Smith, K. M. *Tetrahedron Lett.* **1994**, *35*, 7581. (g) Barkigia, K. M.; Fajer, J.; Berber, M. D.; Smith, K. M. *Acta Crystallogr., Sect. C* **1995**, *C51*, 511.

(21) Monoquaternized porphyrins: (a) Hirayama, N.; Takenaka, A.; Sasada, Y.; Watanabe, E.-I.; Ogoshi, H.; Yoshida, Z.-I. *J. Chem. Soc., Chem. Commun.* **1974**, 330. (b) Hrung, C. P.; Tsutsui, M.; Cullen, D. L.; Meyer, E. F., Jr.; Morimoto,C. N. *J. Am. Chem. Soc.* **1978**, *100*, 6068. (c) Hirayama, N.; Takenaka, A.; Sasada, Y.; Watanabe, E. *Bull. Chem. Soc. Jpn.* **1981**, *54*, 998. (d) Lavallee, D. K.; Anderson, O. P. *J. Am. Chem. Soc.* **1982**, *104*, 4707. (e) Balch, A. L.; Chan, Y. W.; Olmstead, M.; Renner, M. W. *J. Am. Chem. Soc.* **1985**, *107*, 2393. (f) McLaughlin, G. M. *J. Chem. Soc., Perkin Trans. 2* **1974**, 136. (g) Goldberg, D. E.; Thomas, K. M. *J. Am. Chem. Soc.* **1976**, *98*, 913.

(22) *N*,*N*′-Dialkyl and *N*,*N*′-bridged porphyrins: (a) Abeysekera, A. M.; Grigg, R.; Trocha-Grimshaw, J. *Tetrahedron* **1980**, *36*, 1857. (b) Bartczak, T. J. *Acta Crystallogr.* **1985**, *C41*, 604. (c) Callot, H. J.; Cromer, R.; Louati, A.; Metz, B.; Chevrier, B. *J. Am. Chem. Soc.* **1987**, *109*, 2946.

(23) Hamor, M. J.; Hamor, T. A.; Hoard, J. L. *J. Am. Chem. Soc.* **1964**, *86*, 1938.

(24) Hobbs, J. D.; Majumder, S. A.; Luo, L.; Sickelsmith, G. A.; Quirke, J. M. E.; Medforth, C. J.; Smith, K. M.; Shelnutt, J. A. *J. Am. Chem. Soc.* **1994**, *116*, 3261.

(25) (a) Burkert, U.; Allinger, N. L. *J. Comput. Chem.* **1982**, *3*, 40. (b) Wiberg, K. B.; Boyd, R. H. *J. Am. Chem. Soc.* **1972**, *94*, 8426. (c) Person, R. V.; Peterson, B. R.; Lightner, D. A. *J. Am. Chem. Soc.* **1994**, *116*, 42. (d) Beech, J.; Cragg, P. J.; Drew, M. G. B. *J. Chem. Soc., Dalton Trans.* **1994**, 719.

substitution pattern in a class of relatively unstrained porphyrins engenders systematic conformational changes that reflect an underlying change in the inherent flexibility of the ligand. After our structure determinations, but while our MM calculations were in progress, a paper by Senge et al.[20d] appeared that reported several new porphyrin diacid species. We have incorporated those results into our MM calculations. This has led to a new force field, for use with our modified version of MM2(87),[26,27a] specifically developed for porphyrin diacids. The force field has been used to map the process of conformational inversion ($D_{2d} \rightarrow D_{2d}$) in $[H_4\text{porphine}]^{2+}$, $[H_4\text{OEP}]^{2+}$, $[H_4\text{-TPP}]^{2+}$, and $[H_4\text{T-2,6-Cl}_2\text{PP}]^{2+}$ in an attempt to determine the relative flexibilities of these species from their *in vacuo* strain energy barriers. Molecular mechanics methods have also been used to delineate the role played by peripheral group−porphyrin nonbonded interactions in determining the relative flexibilities of *meso*-tetraaryl porphyrin diacids.

Experimental Section

General Information. Dichloromethane, hexane, benzene, and sodium sulfate were purchased from Fisher and 70% perchloric acid was obtained from Aldrich. H_2OEP was purchased from Midcentury Chemicals; H_2TPP[28] and H_2TMP[29] were synthesized following literature methods. IR spectra were determined as KBr pellets on a Perkin Elmer 883 spectrometer, and electronic spectra were recorded on a Perkin Elmer Lambda 19 UV/vis/near-IR spectrometer.

Synthesis of Porphyrin Diacids. All three diacid species can be prepared by acid treatment of the porphyrin free base. Two hundred milligrams of H_2OEP, H_2TPP, or H_2TMP was dissolved in 20 mL of dichloromethane, ∼5 mL of concentrated perchloric acid was added, and the mixture was stirred for 30 min. The solution of H_2OEP turned red-purple, while the solutions of H_2TPP and H_2TMP turned grass green. Electronic spectra did not show the characteristic four-banded porphyrin free base pattern.[1] The dichloromethane phase was separated and dried with anhydrous sodium sulfate, the drying agent was removed by filtration, the residual protonated compound washed out of the fritted-glass filter with dichloromethane, and the solution evaporated to dryness. For $[H_4\text{TMP}]^{2+}$ we also used a slightly modified synthesis starting from [Zn(TMP)]. Treatment of [Zn(TMP)] with an excess of concentrated acid leads to demetalation, followed by protonation of the pyrrole nitrogen atoms to form the diacid species. Spectra for $[H_4\text{OEP}](ClO_4)_2$: IR (ν ClO_4), 1119(s), 1091(s), 626(m) cm^{-1}; UV−vis (CH_2Cl_2), 403, 550, 592 nm; $[H_4\text{TPP}](ClO_4)_2$: IR (ν ClO_4), 1130(sh), 1094(s), 629(m) cm^{-1}; UV−vis (CH_2Cl_2), 439, 602, 655 nm; $[H_4\text{TMP}](ClO_4)_2$: IR (ν ClO_4), 1140(s), 1122(sh), 1109(sh), 1091(sh), 624(m) cm^{-1}; UV−vis (CH_2Cl_2), 436, 583, 632 nm. *Caution!* Although we have encountered no problems with the above procedures for the preparation of perchlorate salts of porphyrin diacids, they are potentially unstable and may decompose spontaneously upon exposure to heat or if mechanically shocked. All perchlorate salts should be handled with care in milligram quantities.

Crystallization of Porphyrin Diacids. Forty milligrams of $[H_4\text{OEP}](ClO_4)_2$ was dissolved in 2 mL of CH_2Cl_2 and layered with hexane. After 3 days, pink plate- and diamond-shaped crystals were harvested; although the latter were twinned, the plate-shaped crystals were suitable for single-crystal X-ray analysis. Green needle-shaped crystals of $[H_4\text{-TPP}](ClO_4)_2\cdot C_6H_6$ were crystallized by slow vapor diffusion of benzene into 4 mL of CH_2Cl_2 containing 40 mg of $[H_4\text{TPP}](ClO_4)_2$. (In our laboratory, CH_2Cl_2 and benzene were the only pair of solvents that afforded X-ray quality crystals of $[H_4\text{TPP}](ClO_4)_2$.) Fifty milligrams of $[H_4\text{TMP}](ClO_4)_2$ was dissolved in 2 mL of a 3:1 mixture of CH_2Cl_2 and ethanol and layered with hexane. After 1 week, green plate-like crystals were obtained. In our experience, the presence of ethanol is necessary to get X-ray quality crystals.

X-ray Structure Determinations. X-ray diffraction data were collected on an Enraf-Nonius FAST area-detector diffractometer with a Mo rotating anode source ($\bar{\lambda} = 0.71073$ Å). Our detailed methods and procedures for small molecule X-ray data collection have been described previously.[19] Data were corrected for Lorentz and polarization factors, and, at the final stage, a modified version[30] of the absorption correction program DIFABS was applied.

All three structures were solved with SHELXS-86;[31] the remaining non-hydrogen atoms were located by difference Fourier syntheses. Structures were refined against F^2 with SHELXL-93.[32] All data collected were used including negative intensities. Almost all porphyrin hydrogen atoms were located in difference Fourier maps and, except for those bonded to the pyrrole nitrogen atoms, were included as idealized contributors in the least-squares process. Standard SHELXL-93 idealization parameters were used. All the hydrogens bonded to the pyrrole nitrogen atoms were located in difference Fouriers. The coordinates of these atoms and isotropic temperature factors were refined in all subsequent least-squares cycles. The one exception was atom H(4) in $[H_4\text{TPP}]^{2+}$, where the thermal parameter became unreasonably small, but whose geometry remained as good as that of the other three hydrogen atoms. Therefore, the thermal parameter of this atom was fixed with a U value of 0.030 (equal to the smallest U value found for the other three hydrogen atoms), and only its coordinates were refined.

$[H_4\text{OEP}](ClO_4)_2$ was found to form a nonsolvated lattice and $[H_4\text{-TPP}](ClO_4)_2$ was found to have a well-behaved benzene molecule of crystallization. Crystalline $[H_4\text{TMP}](ClO_4)_2$ had an ethanol molecule of solvation disordered around an inversion center; some effort was required to find a satisfactory crystallographic model. The perchlorate anions in this structure are also disordered. Two types of well-resolved disorder were observed: either a rotational disorder about the Cl−O bond to the oxygen atom hydrogen bonded to the pyrrole NH hydrogen atom, or a "rocking" disorder in which two or three oxygen atoms and the chlorine each occupy two distinct positions. In both cases, the oxygen atom that is hydrogen bonded to a pair of porphyrin NH protons is totally ordered. At the final stage of the refinement for $[H_4\text{TMP}](ClO_4)_2$, a peak with a height of 1.26 e/Å^3 located in the center of the porphyrin core of molecule **2** was evaluated. This small peak was interpreted as a minor amount (no higher than 2%) of a Zn^{2+} impurity in one of the two independent molecules in the asymmetric unit. Although the amount of this impurity is small, its presence appeared to have a significant effect on the crystal size.

Complete crystallographic details, fractional atomic coordinates for all non-hydrogen atoms and the four porphyrin NH hydrogens, anisotropic thermal parameters, and fixed hydrogen atom coordinates for each structure are given in the Supporting Information.

$[H_4\text{OEP}](ClO_4)_2$: $C_{36}H_{48}N_4O_8Cl_2$, fw = 735.74 amu, a = 17.221(4) Å, b = 13.147(1) Å, c = 17.332(3) Å, β = 106.29(1)°, V = 3766.5(11) Å^3, monoclinic, space group $P2_1/n$, Z = 4, ρ_{calc} = 1.297 g/cm^3, μ = 0.227 mm^{-1}, T = 127(1) K, R_1 = 0.069 for 5,457 "observed" data with $F_o \geq 4.0\sigma(F_o)$,[33] and wR_2 = 0.190 for 9454 unique data.

$[H_4\text{TPP}](ClO_4)_2\cdot C_6H_6$: $C_{50}H_{38}N_4O_8Cl_2$, fw = 893.74 amu, a = 8.033(4) Å, b = 31.015(13) Å, c = 16.897(4) Å, β = 98.65(3)°, V = 4162(3) Å^3, monoclinic, space group $P2_1/c$, Z = 4, ρ_{calc} = 1.389 g/cm^3, μ = 0.215 mm^{-1}, T = 127(1) K, R_1 = 0.107 for 3652 observed data with $F_o \geq 4.0\sigma(F_o)$, and wR_2 = 0.274 for 9686 total data.

$[H_4\text{TMP}](ClO_4)_2\cdot{}^1/_2\text{EtOH}$: $C_{57}H_{59}N_4O_{8.5}Cl_2$, fw = 1007.03 amu, a = 14.288(3) Å, b = 19.153(11) Å, c = 19.622(9) Å, α = 97.80(1)°, β = 99.16(2)°, γ = 98.12(2)°, V = 5179(4) Å^3, triclinic, space group $P\bar{1}$, Z = 4, ρ_{calc} = 1.291 g/cm^3, μ = 0.181 mm^{-1}, T = 127(1) K, R_1 = 0.080 for 15339 observed data with $F_o \geq 4.0\sigma(F_o)$, and wR_2 = 0.211 for 26150 unique data.

(26) Munro, O. Q.; Bradley, J. C.; Hancock, R. D.; Marques, H. M.; Marsicano, F.; Wade, P. W. *J. Am. Chem. Soc.* **1992**, *114*, 7218.

(27) (a) Munro, O. Q.; Marques, H. M.; Debrunner, P. G.; Mohanrao, K.; Scheidt, W. R. *J. Am. Chem. Soc.* **1995**, *117*, 935. (b) Marques, H. M.; Munro, O. Q.; Grimmer, N. E.; Levendis, D. C.; Marsicano, F.; Pattrick, G.; Markoulides, T. *J. Chem. Soc., Faraday Trans.* **1995**, *91*, 1741.

(28) Longo, F. R.; Finarelli, J. D.; Goldmacher, J.; Assour, J.; Korsakoff, L. *J. Org. Chem.* **1967**, *32*, 476.

(29) (a) Wagner, R. W.; Lawrence, D. S.; Lindsey, J. S. *Tetrahedron Lett.* **1987**, *28*, 3069. (b) Lindsey, J. S.; Wagner, R. W. *J. Org. Chem.* **1988**, *54*, 828.

(30) (a) The process is based on an adaptation of the DIFABS[30b] logic to area detector geometry by Karaulov: Karaulov, A. I.; School of Chemistry and Applied Chemistry, University of Wales, College of Cardiff, Cardiff CF1 3TB, UK; personal communication. (b) Walker, N. P.; Stuart, D. *Acta Crystallogr., Sect. A* **1983**, *A39*, 158.

(31) Sheldrick, G. M. *Acta Crystallogr., Sect. A* **1990**, *A46*, 467.

(32) Sheldrick, G. M. *J. Appl. Cryst.*, manuscript in preparation.

Molecular Mechanics Calculations. These were performed on an IBM compatible computer with our modified version[26] of Allinger's MM program MM2(87).[34] ALCHEMY III[35] was used for molecule building and viewing. A cut-off criterion for energy minimization of $\Delta U_T \leq 0.000\,060$ kcal/mol between successive iterations was used. With different starting geometries for refinement, the total steric energies calculated were reproducible to within 0.0003−0.001 kcal/mol. A dielectric constant of 10 D was used throughout to take into account a fairly polar crystal environment. Point charges were not used in the calculations.[36]

Porphyrin diacid force field parameters were derived from those for low-spin iron(III) porphyrins.[27a] The barrier heights of some of the porphyrin core torsional parameters were reduced to 93% ($N_p-C_a-C_m-C_a$), 39% ($C_a-N_p-C_a-C_b$), and 24% ($C_a-N_p-C_a-C_m$) of the stiffness appropriate for low-spin ferric porphyrins.[37] The crystal structures of $[H_4OEP](ClO_4)_2$, $[H_4TMP](ClO_4)_2$, and $[H_4TPP](ClO_4)_2$ were used initially for parametrization of the force field[38] and, subsequently, the highly distorted X-ray structure of $[H_4OETPP](OAc)_{3/2}(TFA)_{1/2}$.[20d] Counterions were not included in the calculations. New parameters for protonated pyridyl groups were developed from the X-ray data for $[H_2TPyP]\cdot 6HCl$.[20b] Comparisons of MM-calculated and crystallographically observed bond lengths, bond angles, and torsion angles are given in the Supporting Information. New force field parameters and MM2 atom types are given in Table S43 and Figure S5, respectively.

MM2's torsion angle driving algorithm was used to map conformational inversion in $[H_4porphine]^{2+}$, $[H_4OEP]^{2+}$, $[H_4TPP]^{2+}$, and $[H_4T\text{-}2,6\text{-}Cl_2PP]^{2+}$.[39] Selected pairs of opposite $N-C_a-C_m-C_a$ torsion angles (Ψ_1 and Ψ_2) were driven from −30° to 30° in 3° increments. Planar structures with D_{4h} symmetry were used as starting conformations on the 21 × 21 grid of conformational space. The method used by MM2 to fix the driven torsion angles has been described elsewhere.[27a] The strain energy components of the energy-optimized conformations were extracted from the MM2 output files and analyzed as a function of the driven torsion angles. The calculations were confined to these four porphyrin diacids since their free bases[40,41] are planar and the perturbation introduced by protonating the four porphyrin nitrogens will be approximately constant across the whole series; this is not expected to be the case with species such as $[H_4OBrTPP]^{2+}$ (highly saddled free base).[42]

In a second series of calculations aimed at exploring molecular flexibility along a reaction coordinate defined by the orientations of the *meso*-aryl groups, torsion angles involving the four aryl substituents ($C_a-C_m-C_p-C_p$, χ) in $[H_4TPyP]^{2+}$, $[H_4TPP]^{2+}$, $[H_4T\text{-}2,6\text{-}(OH)_2PP]^{2+}$, $[H_4T\text{-}2,6\text{-}F_2PP]^{2+}$, $[H_4T\text{-}2,6\text{-}Cl_2PP]^{2+}$, and $[H_4TMP]^{2+}$ were driven from ∼115° to ∼25° in 5° steps, maintaining near D_{2d} symmetry throughout.[43] Steric energy components and atomic displacements from the 24-atom porphyrin mean plane were analyzed as a function of the mean aryl group orientation, χ_{av}.

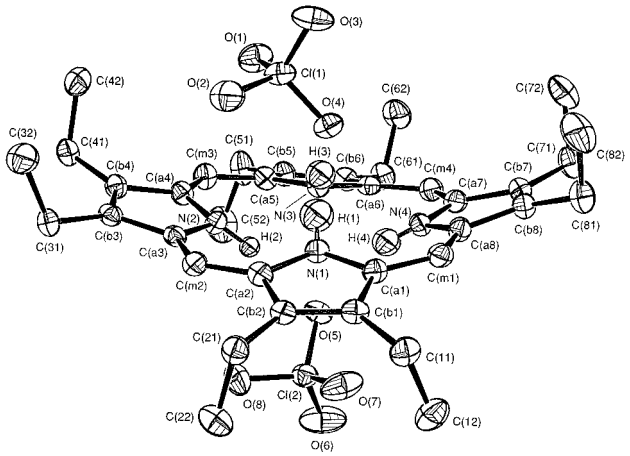

Figure 1. ORTEP diagram of the structure of $[H_4OEP](ClO_4)_2$. Thermal ellipsoids are drawn at the 50% probability level. The refined positions of the hydrogen atoms bonded to the pyrrole nitrogens are shown; all other hydrogen atoms have been omitted for clarity.

Results

Molecular Structures. ORTEP diagrams of $[H_4OEP](ClO_4)_2$ and $[H_4TMP](ClO_4)_2$ (molecule **1**) are presented in Figures 1 and 2. Also illustrated in these diagrams are the labeling scheme used in the tables for the non-hydrogen atoms. The ORTEP diagrams of $[H_4TPP](ClO_4)_2$ and molecule **2** of $[H_4TMP](ClO_4)_2$ are included in the Supporting Information. In the tables for $[H_4TMP](ClO_4)_2$, the atom names of molecule **1** are preceded by the numeral "1" and those of molecule **2** by "2"; however, these indices are omitted in their ORTEP diagrams. All ORTEP diagrams illustrate the experimentally derived positions of the four inner hydrogen atoms of the diacid derivatives. The

(33) $R_1 = \sum||F_o| - |F_c||/\sum|F_o|$ and $wR_2 = \{\sum[w(F_o^2 - F_c^2)^2]/\sum[wF_o^4]\}^{1/2}$. R factors R_1 are based on F, with F set to zero for negative F^2. The criterion of $F^2 > 2\sigma(F^2)$ was used only for calculating R_1. R factors based on F^2 (wR_2) are statistically about twice as large as those based on F.

(34) (a) Allinger, N. L. *J. Am. Chem. Soc.* **1977**, *99*, 8127. (b) Allinger, N. L.; Yuh, Y. MM2(87). Distributed to academic users by QCPE, under special agreement with Molecular Design Ltd., San Leandro, CA. (c) Sprague, J. T.; Tai, J. C.; Young, Y.; Allinger, N. L. *J. Comput. Chem.* **1987**, *8*, 581. (d) Burkert, U.; Allinger, N. L. *Molecular Mechanics*; ACS Monograph 177, American Chemical Society: Washington, DC, 1982. (e) Bowen, J. P.; Allinger, N. L. In *Reviews in Computational Chemistry*; Lipkowitz, K. B., Boyd, D. B., Eds.; VCH Publishers: New York, 1991; Vol. 2, p 81.

(35) ALCHEMY III, 3D Molecular Modeling Software; Tripos Associates Inc. Other programs used in this study: (1) XANADU; Roberts, P.; Sheldrick, G. M. 1976/7. (Used to fit least-squares planes through the Cartesian coordinates of calculated structures.) (2) AXUM; Technical Graphics and Data Analysis (V. 3.0), TriMetrix Inc. (3) SCHAKAL 88, Program for the Graphic Representation of Molecular and Crystallographic Models; Keller, E. Kristallographisches Institut der Universität, Hebelstr. 25, D-7800, Freiburg, Germany.

(36) (a) Since the extent of charge delocalization over the porphyrin skeleton is unknown, and likely to be porphyrin dependent, localized point charges were not used in the calculations. We,[26,27] and others,[36b] have found that good structural models of metalloporphyrin cations may be obtained even if the electrostatic component of the total steric energy is ignored. The empirical force field for porphyrin diacids therefore neglects charge but not dipole contributions to the core geometry. (b) Shelnutt, J. A.; Medforth, C. J.; Berber, M. D.; Barkigia, K. M.; Smith, K. M. *J. Am. Chem. Soc.* **1991**, *113*, 4077.

(37) The force field for porphyrin diacids was tested on the structure of $[Fe(TMP)(1,2\text{-}Me_2\text{-}Im)_2]ClO_4$;[27a] although an improved fit of the porphyrin core conformation (S_4-ruffling) was obtained (rmsd = 0.047 Å vs 0.060 Å), the mean $Fe-N_p$ bond distance was calculated to be too long by 0.037 Å. This suggests that a degree of cross-correlation between the bond stretching and torsional parameters for the coordinated metal ion exists and, presumably, that more than one set of parameters could describe the same class of structures.

(38) Acceptable rmsd's (bond lengths, bond angles, torsion angles, 24-atom core) were obtained with the calculated and X-ray structures: $[H_4TMTEP](ClO_4)_2$[20d,f] (0.014(10) Å, 0.5(3)°, 1.8(9)°, 0.062 Å); $[H_4OEP](ClO_4)_2$ (0.008(7) Å, 0.6(5)°, 1.8(1.3)°, 0.093 Å); $[H_4TMP](ClO_4)_2$ (0.010(5) Å, 0.81(83)°, 0.9(6)°, 0.038 Å); $[H_2TPyP]\cdot 6HCl$[20b] (0.009(7) Å, 0.7(6)°, 1.5(9)°, 0.100 Å); $[H_4TPP](ClO_4)_2$ (0.010(9) Å, 0.4(4)°, 1.3(1.4)°, 0.091 Å); $[H_4OETPP](OAc)_{3/2}(TFA)_{1/2}$[20d] (0.010(4) Å, 0.5(6)°, 2.5(2.1)°, 0.088 Å); and $[H_4OBrTPP](TFA)_2$[20d] (0.017(8) Å, 0.7(5)°, 2.7(3.0)°, 0.078 Å).

(39) Since MM2 is dimensioned to drive a maximum of 50 atoms per dihedral angle for intraring torsion angles and $[H_4TMP]^{2+}$ exceeds this limit, $[H_4T\text{-}2,6\text{-}Cl_2PP]^{2+}$ was used in its place. (Derivatives of TMP show near-identical steric properties to those of T-2,6-Cl_2PP.[27a])

(40) Free base porphyrins: (a) Codding, P. W.; Tulinsky, A. *J. Am. Chem. Soc.* **1972**, *94*, 4151. (b) Silvers, S. J.; Tulinsky, A. *J. Am. Chem. Soc.* **1967**, *89*, 3331. (c) Chen, B. M. L.; Tulinsky, A. *J. Am. Chem. Soc.* **1972**, *94*, 4144. (d) Lauher, J. W.; Ibers, J. A. *J. Am. Chem. Soc.* **1973**, *95*, 5148. (e) Little, R. G.; Ibers, J. A. *J. Am. Chem. Soc.* **1975**, *97*, 5363. (f) Caughey, W. S.; Ibers, J. A. *J. Am. Chem. Soc.* **1977**, *99*, 6639.

(41) Ochsenbein, P.; Ayougou, K.; Mandon, D.; Fischer, J.; Weiss, R.; Austin, R. N.; Jayaraj, K.; Gold, A.; Terner, J.; Fajer, J. *Angew. Chem., Int. Ed. Engl.* **1994**, *33*, 48.

(42) Bhyrappa, P.; Nethaji, M.; Krishnan, V. *Chem. Lett.* **1993**, 869.

(43) Because a maximum of two torsion angles may be driven at a time by conventional conformational mapping methods, the orientations of the four aryl groups were varied by (i) carrying out a constraint-free geometry optimization, (ii) setting the four dihedral angles to a particular value in the 25−115° range (retaining the D_{2d} symmetry of the molecule), (iii) constraining the four porphyrin−*meso*-aryl group torsion angles ($C_a-C_m-C_p-C_p$) by restricting translation of each set of four atoms in the *x*-, *y*-, and *z*-directions, and (iv) refining the geometry of the conformation.

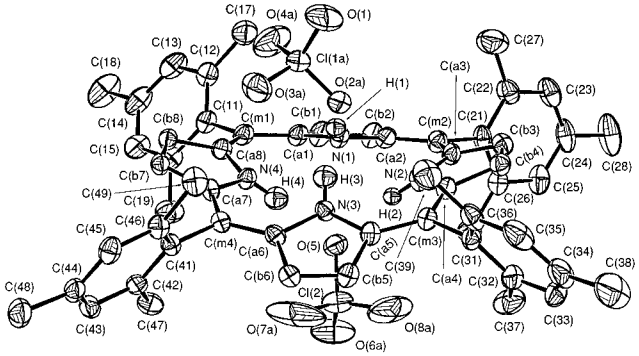

Figure 2. ORTEP diagram of the structure of $[H_4TMP](ClO_4)_2$ (molecule **1**). The same information is given as in Figure 1.

diagrams clearly show that in each derivative the perchlorate ions form hydrogen bonds to the protons of the porphyrin diacid. The small thermal parameter values of the hydrogen-bonded oxygen atom, relative to the other oxygen atoms of the perchlorate ions and visible in the ORTEP diagrams, is clear evidence for the hydrogen bonding interaction. In the three structures the H···O distances (based on the refined hydrogen atom positions) range from 1.94 to 2.24 Å. Values of the N−H···O angles were close to linear with values in the range 160−179°. The average values for H···O distances (or N−H···O angles) in each of the derivatives are 2.09 Å (165°) in $[H_4OEP](ClO_4)_2$, 2.12 Å (165°) in $[H_4TPP](ClO_4)_2$, and 2.00 Å (170°) in $[H_4TMP](ClO_4)_2$ (molecule **1**) and 1.99 Å (172°) (molecule **2**).

The ORTEP diagrams clearly show the distortion from planarity that results from the severe transannular crowding between the four hydrogen atoms of the pyrrole nitrogen atoms. Each derivative shows a distinct D_{2d}-saddled porphyrin core. The β-carbon atoms of each pyrrole are alternately displaced above and below the mean porphyrin plane (Figure 3). The magnitudes can be seen in Figure 3, which are formal diagrams that show the perpendicular displacement of each atom (in units of 0.01 Å) from the mean plane of the 24-atom core. Displacements of the four central hydrogen atoms are also shown in these diagrams. The deviation from planarity in the three derivatives can be measured by the average absolute perpendicular displacement of the beta carbon atoms from the respective 24-atom mean plane and follows the order $[H_4OEP](ClO_4)_2$ (0.46(7) Å) < $[H_4TMP](ClO_4)_2$ (molecule **2**, 0.61(5) Å) ≈ $[H_4TMP](ClO_4)_2$ (molecule **1**, 0.67(3) Å) ≪ $[H_4TPP](ClO_4)_2$ (0.93(6) Å). The numbers in parentheses following each absolute average is the esd; the small values show the small dispersion of the individual atomic displacements. The pyrrole NH protons are also alternately displaced above and below the 24-atom mean plane; individual pyrrole−24-atom core dihedral angles for each pyrrole ring are listed in Table 1.

Individual *meso*-aryl group−porphyrin dihedral angles range between 23.4−87.0° (Table 1). The four phenyl group−porphyrin dihedral angles in $[H_4TPP](ClO_4)_2$ are quite acute, averaging only 27(2)°. The mesityl group−porphyrin dihedral angles of the two independent molecules of $[H_4TMP](ClO_4)_2$, on the other hand, are much larger, averaging 63(13)° in molecule **1** and 75(15)° in molecule **2**. The large esd's in parentheses show the considerable variation in the mesityl group−porphyrin dihedral angles. The magnitude of the saddle distortion in the three *meso*-tetraaryl porphyrin diacid derivatives (Figure 3) clearly increases with decreasing *meso*-aryl group−porphyrin dihedral angle, as demonstrated previously.[17,26]

Individual bond distances and bond angles for the three structures are given in the Supporting Information. Averaged values for the unique chemical classes of distances and angles in the porphinato cores of the four dications are entered on their mean plane diagrams given in Figure 3.

Molecular Mechanics. Calculated and crystallographically observed core conformations for *meso*-tetraaryl porphyrin diacids are compared in Table 2.[44] Two calculated structures are given. The first was obtained by constraining the four aryl group orientations at their X-ray values during refinement (accounting for the influence of packing constraints on the conformation). Core conformations calculated by this method match those of the X-ray structures. The second calculated structure is that produced without geometry constraints; these "gas-phase" conformations[45] are considerably less saddled than the X-ray structures. The unconstrained conformations of $[H_4TPP]^{2+}$, $[H_4TPyP]^{2+}$, and $[H_4TMP]^{2+}$ show similar D_{2d} symmetry core distortions: $|N_4|$ ∼0.13 Å, $|C_a|$ ∼0.12 Å, $|C_b|$ ∼0.49 Å, $|C_m|$ ∼0−0.07 Å, and $|C_{20}|$ ∼0.25 Å, with χ_{av} ∼85°. The total strain energy *difference* between the "gas-phase" conformation and that modeling the X-ray structure ranges from 5.94 kcal/mol in $[H_4TMP]^{2+}$ to 20.87 kcal/mol in $[H_4OBrTPP]^{2+}$, with the less distorted structure lowest in energy in each case.

Analogous data for β-alkyl porphyrin diacids are compared in Table 3. All calculated structures, with the exception of the D_{4h} conformation of $[H_4porphine]^{2+}$, were obtained without geometry constraints. The agreement between the calculated and observed core conformations of $[H_4OEP](ClO_4)_2$ and $[H_4TMTEP](ClO_4)_2$[20d,f] is particularly good. However, the calculated structure of $[H_4TCHP]^{2+}$ is less distorted than the X-ray structure[20d] since it has C_{2h}[46] rather than C_{2h}' symmetry.

$[H_4OEP](ClO_4)_2$ (Figure 1) has the ethyl group configuration $-++--++-$, where the signs denote methyl group orientations above (+) and below (−) the plane of the pyrrole ring. From Table 3, different ethyl group configurations perturb the D_{2d}-saddled conformation of the porphyrin core[47] and determine the energy of the configurational isomer. (The $-+-+-+-+$ isomer is lowest in energy and the $--++--++$ isomer the least stable by 1.41 kcal/mol.[48]) $[H_4TMTEP]^{2+}$ shows smaller peripheral group-dependent variations in core conformation.

Figure 4 shows plots of the change in total steric energy (ΔU_T) as a function of the torsion angles Ψ_1 and Ψ_2 for $[H_4porphine]^{2+}$, $(+-+-+-+-)$ $[H_4OEP]^{2+}$,[49] $[H_4TPP]^{2+}$, and $[H_4T\text{-}2,6\text{-}Cl_2PP]^{2+}$.[50] In each case, two D_{2d} symmetry global minima (related by a center of inversion at 0°,0°) occur at $\Psi_1,\Psi_2 = -12°, -12°$ and 12°,12°. An inversion related pair of C_{2h} conformations have coordinates $\Psi_1,\Psi_2 = -21°$, 21° and 21°,

(44) Calculated and observed structures are also compared in Figure S8. The calculated structures of the *meso*-tetraaryl porphyrin diacids were obtained by fixing the orientations ($C_a-C_m-C_p-C_p$, χ) of the aryl groups at their X-ray values. All bond lengths, bond angles, and torsional angles (other than χ) were fully optimized during structural refinement.

(45) Since the force field has been parametrized using crystallographic data, unconstrained conformations may not represent the gas phase if the crystallographic structures are strongly affected by environmental effects.

(46) The calculated conformation with C_{2h} core symmetry has one pair of opposite pyrrole rings approximately in the 24-atom mean plane and the NH groups of the second pair of pyrrole rings canted above and below the mean plane. The X-ray structure displays effective C_{2h}' symmetry with one adjacent pair of pyrrole NH groups displaced above the 24-atom mean plane and the second (opposite) pair below the porphyrin mean plane, producing a discrete step in the core geometry.

(47) In $[H_4OEP]^{2+}$, the mean absolute perpendicular displacements of the various classes of porphyrin core atoms span the ranges 0.11−0.15 Å (pyrrole nitrogens), 0.07−0.12 Å (C_a), 0.38−0.49 Å (C_b), and ∼0 Å (C_m).

(48) For a two-state system, energy differences of 0.5, 1.0, and 1.5 kcal/mol would lead to lower-state populations of 70, 84, and 93%, respectively, at 298 K.

(49) The $(+-+-+-+-)$ isomer of $[H_4OEP]^{2+}$ was used in this study to ensure inversion symmetry upon reflection of the configuration through the porphyrin mean plane.

(50) Ψ_1 and Ψ_2, which define the internal reaction coordinate, are a pair of intra-ring $N-C_a-C_m-C_a$ torsion angles related by a C_2 axis along the porphyrin normal.

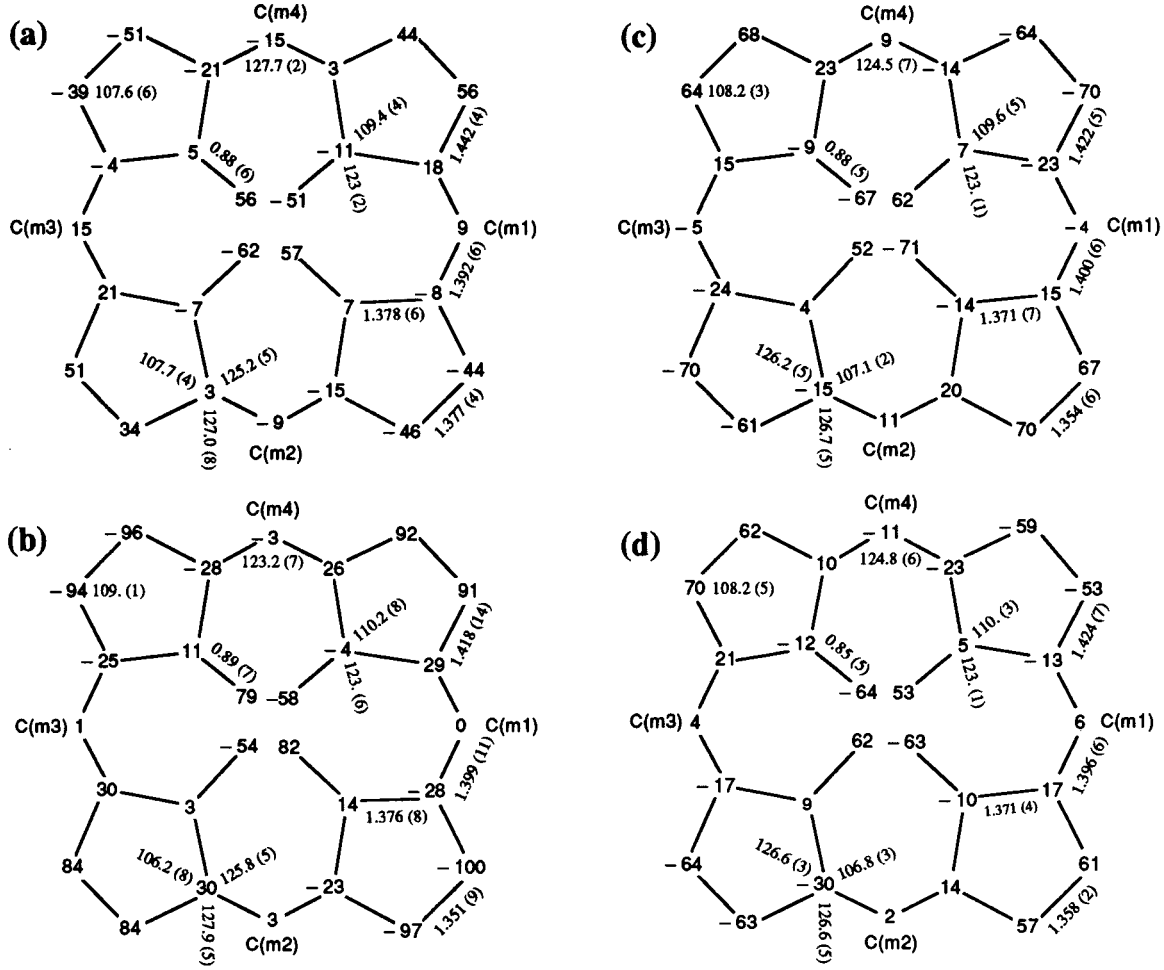

Figure 3. Formal diagrams of the porphyrin diacid cores of (a) $[H_4OEP](ClO_4)_2$, (b) $[H_4TPP](ClO_4)_2$, (c) $[H_4TMP](ClO_4)_2$ (molecule **1**), and (d) $[H_4TMP](ClO_4)_2$ (molecule **2**). Averaged values of the chemically unique bond distances (in Å) and angles (in deg) are shown. The numbers in parentheses are the esd's calculated on the assumption that the averaged values were all drawn from the same population. The perpendicular displacements (in units of 0.01 Å) of the porphyrin core atoms from the 24-atom mean plane are also displayed.

Table 1. Pyrrole−Porphyrin and Aryl Group−Porphyrin Dihedral Angles in $[H_4OEP](ClO_4)_2$, $[H_4TPP](ClO_4)_2 \cdot C_6H_6$, and $[H_4TMP](ClO_4)_2 \cdot {}^1/_2EtOH$[a]

	$[H_4OEP]^{2+}$	$[H_4TPP]^{2+}$	$[H_4TMP]^{2+}$ [b]	$[H_4TMP]^{2+}$ [c]
pyrrole 1	13.88	31.94	22.46	18.80
pyrrole 2	14.03	22.55	19.25	20.09
pyrrole 3	14.20	29.91	20.44	21.73
pyrrole 4	16.94	27.16	20.58	16.87
aryl 1		23.43	52.19	86.95
aryl 2		26.99	82.23	81.66
aryl 3		28.19	57.76	53.51
aryl 4		27.35	58.66	77.59

[a] Dihedral angles in deg. [b] Molecule **1**. [c] Molecule **2.**

−21°. For the four porphyrin diacids studied, the C_{2h} minima lie higher in energy than the D_{2d} minima. The *stability* of the D_{2d} isomer relative to the C_{2h} isomer increases in the order $[H_4$-porphine$]^{2+}$ (≈ −0.8 kcal/mol) < (+ − + − + − + −) $[H_4$-OEP$]^{2+}$ (≈ −1.0 kcal/mol) < $[H_4TPP]^{2+}$ (−1.7 kcal/mol) < $[H_4$T-2,6-Cl_2PP$]^{2+}$ (−1.8 kcal/mol).

The calculated barrier to conformational inversion between the pair of D_{2d} isomers for $[H_4$porphine$]^{2+}$, (+ − + − + − + −) $[H_4OEP]^{2+}$, and $[H_4TPP]^{2+}$ (Figure 4) is located at a saddle point with C_{2v} symmetry ($\Psi_1,\Psi_2 = 0°,0°$). The C_{2v} conformation for $[H_4$T-2,6-Cl_2PP$]^{2+}$ lies atop a knoll flanked by a pair of isoenergetic cols ($\Psi_1,\Psi_2 = -4°,4°$ and $4°,-4°$).[51] Selected conformations of $[H_4TPP]^{2+}$ taken from Figure 4, including the C_{2v} transition state, are shown in Figure S9. From Figure 4, the calculated strain energy barriers to conformational inversion increase in the order $[H_4$porphine$]^{2+}$ (0.45 kcal/mol) < $[H_4OEP]^{2+}$ (0.55 kcal/mol) < $[H_4TPP]^{2+}$ (1.0 kcal/mol) < $[H_4$T-2,6-Cl_2PP$]^{2+}$ (1.9 kcal/mol).

Figures 5a−c plot the change in nonbonded, torsional, and total steric energy with average *meso*-aryl group orientation, χ_{av}, for $[H_4TPP]^{2+}$, $[H_4TPyP]^{2+}$, $[H_4$T-2,6-F_2PP$]^{2+}$, $[H_4$T-2,6-Cl_2PP$]^{2+}$, and $[H_4$T-2,6-$(OH)_2$PP$]^{2+}$. The minimum in the plot of ΔU_T against χ_{av} gives the optimum aryl group orientation. The general steepness of the relationship between ΔU_T and χ_{av} (Figure 5c) increases in the order $[H_4TPyP]^{2+} \approx [H_4TPP]^{2+} <$ $[H_4$T-2,6-F_2PP$]^{2+} \approx [H_4$T-2,6-$(OH)_2$PP$]^{2+} <$ $[H_4$T-2,6-Cl_2PP$]^{2+}$ $\approx [H_4TMP]^{2+}$, consistent with the increase in peripheral group steric bulk and the extent of porphyrin core distortion (Figure S10). Selected conformations of $[H_4TMP]^{2+}$ lying along the reaction coordinate are shown in Figure S11.

Discussion

All three porphyrin diacid derivatives display a D_{2d}-distortion of the porphyrin core in the solid. The distortions differ substantially and follow the order $[H_4OEP](ClO_4)_2$ ($|C_b| = 0.45$ Å), $[H_4TMP](ClO_4)_2$ ($|C_b| = 0.67$ Å), and $[H_4TPP](ClO_4)_2$ ($|C_b| = 0.93$ Å). Since $[H_4OEP]^{2+}$ is calculated to be modestly less distorted (less flexible) than $[H_4TPP]^{2+}$ and $[H_4TMP]^{2+}$ (Tables 2 and 3) but is *significantly* less distorted than these derivatives in the solid state, it is evident that environmental effects directly influence the degree of distortion. We have therefore used molecular mechanics methods to aid our understanding of the solid-state structures, because the *in vacuo* conformations calculated using this technique are free from environmental constraints.

The structure of $[H_4TPP](ClO_4)_2$ (Figure S6) shows a strongly saddled porphyrin core conformation, acute porphyrin−phenyl

Table 2. Crystallographically Observed and Calculated Porphyrin Diacid Core Conformations (*meso*-Tetraaryl Derivatives with D_{2d} Symmetry)

porphyrin diacid	$\|N_4\|$[a]	$\|C_a\|$[a]	$\|C_b\|$[a]	$\|C_m\|$[a]	$\|C_{20}\|$[a]	$\|C_{20}N_4\|$[a]	χ_{av}[b]	U_T[c]
$[H_4OBrTPP](TFA)_2$[d]	3(2)	52(2)	152(2)	3(1)	82(61)	69(64)	37(1)	
$[H_4OBrTPP]^{2+}$ (calc)[e]	*7(6)*	*48(2)*	*152(6)*	*3(2)*	*81(62)*	*68(63)*	*37(1)*	*26.202*
$[H_4OBrTPP]^{2+}$ (calc)	*6(1)*	*36(1)*	*115(1)*	*1(0)*	*60(47)*	*51(48)*	*67(0)*	*5.335*
$[H_4OETPP](OAc)_{3/2}(TFA)_{1/2}$[d]	2(1)	46(2)	136(2)	3(1)	73(55)	61(57)	54(4)	
$[H_4OETPP](TFA)_2$[f]	1(1)	46(2)	137(2)	3(2)	74(55)	62(57)	54(4)	
$[H_4OETPP]^{2+}$ (calc)[e]	*8(4)*	*43(2)*	*141(2)*	*3(2)*	*74(58)*	*63(59)*	*54(4)*	*−16.345*
$[H_4OETPP]^{2+}$ (calc)	*9(1)*	*38(1)*	*128(1)*	*3(0)*	*67(53)*	*57(53)*	*64(0)*	*−21.264*
$[H_4TPP](ClO_4)_2$	8(5)	28(2)	93(6)	2(2)	48(38)	42(38)	41(2)	
$[H_4TPP](TFA)_2 \cdot [UO_2](TFA)_2$[g]	8(4)	27(4)	90(4)	6(1)	48(36)	41(36)	46(4)	
$[H_4TPP](FeCl_4,Cl)$[h]	5(0)	34(16)	107(11)	28(0)	62(40)	52(42)	36(1)	
$[H_4TPP]^{2+}$ (calc)[e]	*10(5)*	*27(1)*	*96(4)*	*1(1)*	*50(40)*	*43(40)*	*41(2)*	*6.225*
$[H_4TPP]^{2+}$ (calc)	*13(2)*	*12(1)*	*48(1)*	*0(0)*	*24(21)*	*22(19)*	*85(0)*	*−11.389*
$[H_2TPyP] \cdot 6HCl$[h]	11(2)	24(5)	86(4)	6(2)	45(35)	39(35)	45(4)	
$[H_4TPyP]^{2+}$ (calc)[e]	*11(4)*	*24(3)*	*91(3)*	*6(1)*	*47(37)*	*41(37)*	*45(4)*	*27.461*
$[H_4TPyP]^{2+}$ (calc)	*14(0)*	*11(4)*	*49(2)*	*7(0)*	*25(20)*	*23(19)*	*84(1)*	*11.747*
$[H_4TMP](ClO_4)_2$[i]	8(5)	19(5)	67(4)	6(3)	35(27)	31(27)	70(12)	
$[H_4TMP]^{2+}$ (calc)[e]	*10(5)*	*20(6)*	*73(5)*	*5(6)*	*38(30)*	*33(29)*	*70(12)*	*−4.866*
$[H_4TMP]^{2+}$ (calc)	*12(2)*	*13(3)*	*51(2)*	*3(1)*	*26(21)*	*24(20)*	*84(0)*	*−10.809*
$[H_4T\text{-}2,6\text{-}Cl_2PP]^{2+}$ (calc)	*12(1)*	*13(1)*	*50(1)*	*1(0)*	*25(21)*	*23(20)*	*85(0)*	*−2.703*
$[H_4T\text{-}2,6\text{-}(OH)_2PP]^{2+}$ (calc)	*13(0)*	*12(3)*	*49(2)*	*5(0)*	*25(20)*	*23(19)*	*85(0)*	*0.029*
$[H_4T\text{-}2,6\text{-}F_2PP]^{2+}$ (calc)	*13(0)*	*12(0)*	*48(0)*	*0(0)*	*24(21)*	*22(19)*	*85(0)*	*−3.654*

[a] $|C_a|$, $|C_b|$, $|C_m|$, $|C_{20}|$, $|N_4|$, and $|C_{20}N_4|$ are the mean absolute displacements of the α-, β-, *meso*-, 20 porphyrin carbons, pyrrole nitrogens, and 24 core atoms from the 24-atom mean plane of the porphyrin (in units of 0.01 Å), respectively. MM-calculated values are indicated in italics. The values in parentheses are the esd's calculated on the assumption that all averaged values are drawn from the same population. [b] χ_{av} is the average value of the *meso*-aryl group orientation defined by the torsion angle $C_a-C_m-C_p-C_p$, where C_a, C_m, and C_p are α-, *meso*-, and phenyl carbons, respectively. [c] Total steric energy in kcal/mol. [d] Reference 20d. [e] The *meso*-aryl groups were constrained to have the orientations observed in the crystal structure during energy minimization; all other geometric variables were optimized. [f] Reference 20g. [g] Reference 20e. [h] Reference 20b. [i] Molecule **1**.

Table 3. Crystallographically Observed and Calculated Porphyrin Diacid Core Conformations (β-Alkyl Derivatives)

porphyrin diacid	$\|N_4\|$[a]	$\|C_a\|$[a]	$\|C_b\|$[a]	$\|C_m\|$[a]	$\|C_{20}\|$[a]	$\|C_{20}N_4\|$[a]	U_T[b]
$[H_4porphine]^{2+}$ (D_{4h})[c]	*0(0)*	*0(0)*	*0(0)*	*0(0)*	*0(0)*	*0(0)*	*15.211*
$[H_4porphine]^{2+}$ (C_{2h})[d]	*20(22)*	*8(2)*	*14(12)*	*10(0)*	*11(8)*	*12(11)*	*13.190*
$[H_4porphine]^{2+}$ (D_{2d})	*15(0)*	*6(0)*	*34(0)*	*0(0)*	*16(15)*	*16(14)*	*12.428*
$[H_4TCHP](TFA)_2$ (C_{2h}')[e, f]	24(4)	8(5)	16(3)	7(5)	11(6)	13(7)	
$[H_4TCHP]^{2+}$ (C_{2h})[d]	*21(19)*	*8(3)*	*14(11)*	*11(2)*	*11(8)*	*12(11)*	*13.235*
$[H_4TCHP]^{2+}$ (D_{2d})	*15(1)*	*7(0)*	*36(1)*	*0(0)*	*17(16)*	*17(15)*	*12.252*
$[H_4TMTEP](ClO_4)_2$ (+ + + +, D_{2d})[g,h]	7(2)	9(3)	37(4)	4(1)	19(15)	17(15)	
$[H_4TMTEP]^{2+}$ (+ + + +, D_{2d})[h]	*12(4)*	*10(1)*	*43(3)*	*1(1)*	*22(19)*	*20(17)*	*−5.721*
$[H_4TMTEP]^{2+}$ (− + + +, D_{2d})[h]	*13(2)*	*9(1)*	*42(2)*	*1(1)*	*21(18)*	*20(17)*	*−5.942*
$[H_4TMTEP]^{2+}$ (− − + +, D_{2d})[h]	*13(1)*	*8(1)*	*41(1)*	*1(1)*	*20(18)*	*19(16)*	*−5.594*
$[H_4TMTEP]^{2+}$ (− − − +, D_{2d})[h]	*14(2)*	*8(1)*	*40(2)*	*1(1)*	*19(17)*	*18(16)*	*−5.839*
$[H_4TMTEP]^{2+}$ (− − − −, D_{2d})[h]	*14(4)*	*8(1)*	*38(3)*	*1(0)*	*19(17)*	*18(16)*	*−5.517*
$[H_4OEP](TFA)_2$ (− + − − − − − +, D_{2d})[f,h]	31(17)	12(9)	48(13)	28(11)	30(20)	30(19)	
$[H_4OEP]^{2+}$ (− + − − − − − +, D_{2d})[h]	*13(5)*	*10(1)*	*43(4)*	*1(1)*	*21(19)*	*20(17)*	*−10.599*
$[H_4OEP](ClO_4)_2$ (− + + + − − + +, D_{2d})[h]	7(2)	12(8)	45(7)	12(3)	25(18)	22(18)	
$[H_4OEP]^{2+}$(− + + + − − + +, D_{2d})[h]	*15(3)*	*7(1)*	*39(3)*	*2(1)*	*19(17)*	*18(16)*	*−10.039*
$[H_4OEP]^{2+}$ (+ − − − + + − −, D_{2d})[h]	*12(2)*	*12(1)*	*47(2)*	*1(1)*	*24(20)*	*22(19)*	*−10.442*
$[H_4OEP]^{2+}$ (+ + + + + + + +, D_{2d})[h]	*13(11)*	*9(2)*	*42(8)*	*2(0)*	*21(19)*	*20(18)*	*−10.251*
$[H_4OEP]^{2+}$ (+ + − + + + + +, D_{2d})[h]	*13(9)*	*10(2)*	*42(7)*	*1(1)*	*21(19)*	*20(18)*	*−10.481*
$[H_4OEP]^{2+}$ (− − + − − − − −, D_{2d})[h]	*13(9)*	*9(2)*	*40(7)*	*1(1)*	*20(18)*	*19(17)*	*−10.352*
$[H_4OEP]^{2+}$ (+ + − − − − − −, D_{2d})[h]	*12(5)*	*11(1)*	*45(3)*	*1(1)*	*23(20)*	*21(18)*	*−10.168*
$[H_4OEP]^{2+}$(− − + + + + + +, D_{2d})[h]	*14(6)*	*8(1)*	*40(4)*	*1(0)*	*20(18)*	*19(16)*	*−9.903*
$[H_4OEP]^{2+}$(+ + − − + + − −, D_{2d})[h]	*11(1)*	*12(0)*	*49(1)*	*0(0)*	*24(21)*	*22(20)*	*−10.174*
$[H_4OEP]^{2+}$ (− − + + − − + +, D_{2d})[h]	*15(0)*	*7(0)*	*38(0)*	*0(0)*	*18(17)*	*17(15)*	*−9.630*
$[H_4OEP]^{2+}$ (− + − + − + − +, D_{2d})[h]	*13(1)*	*9(1)*	*42(3)*	*0(0)*	*20(18)*	*19(17)*	*−11.041*

[a] $|C_a|$, $|C_b|$, $|C_m|$, $|C_{20}|$, $|N_4|$, and $|C_{20}N_4|$ are the mean absolute displacements of the α-, β-, *meso*-, 20 porphyrin carbons, pyrrole nitrogens, and 24 core atoms from the 24-atom mean plane of the porphyrin (in units of 0.01 Å), respectively. MM-calculated values are indicated in italics. The values in parentheses are the esd's calculated on the assumption that all averaged values are drawn from the same population. [b] Total steric energy in kcal/mol. [c] Conformation calculated by constraining all atoms to be coplanar. [d] Stepped core conformation with one pair of trans pyrrole rings lying in the porphyrin mean plane; the NH groups of the second pair of pyrrole rings are tipped above and below the mean plane. [e] Stepped core conformation with an *adjacent* pair of pyrrole NH groups tipped above the porphyrin mean plane; the other pair of NH groups is canted below the mean plane. [f] Reference 20d. [g] Reference 20f. [h] The + and − signs denote above- and below-plane orientations, respectively, for the CH_3 groups of the ethyl substituents.

dihedral angles (23−28°, Table 1), and bridging hydrogen bonds between each counterion and cofacial pair of trans pyrrole NH protons. The core distortion found in the three X-ray structures of $[H_4TPP]^{2+}$ (Table 2) varies slightly ($|C_b| = 0.90-1.07$ Å) with the average phenyl group orientation; more acute porphyrin−phenyl dihedral angles correlate with larger out-of-plane displacements of the porphyrin β-carbons. This primarily reflects the degree of nonbonded interaction between the phenyl substituents and the flanking pyrrole rings.[17,26] Because the collective peripheral group steric bulk of $[H_4TPP]^{2+}$ is less than that of $[H_4OETPP]^{2+}$ [20d,g] or $[H_4OBrTPP]^{2+}$,[20d] the potential and indeed the observed core distortion is inherently smaller (Table 2).[52] Interestingly, there is no experimental evidence, at least from the $[H_4TPP]^{2+}$ crystal structures, to suggest that the

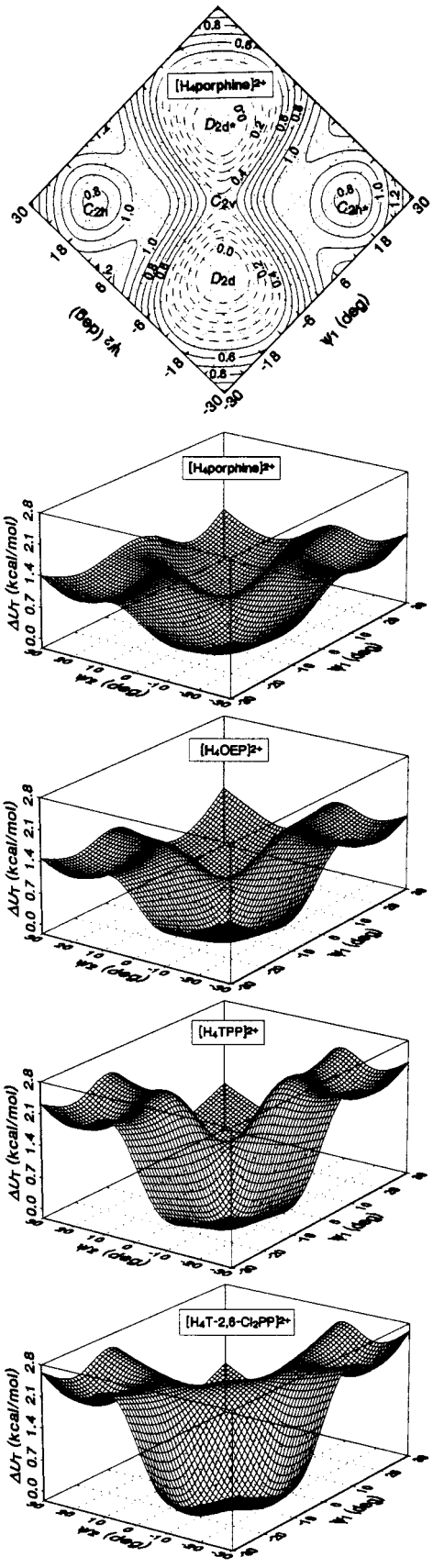

Figure 4. Plots of the change in strain energy relative to the global minimum, ΔU_T, as a function of an opposite pair of N−C_a−C_m−C_a torsion angles, Ψ_1 and Ψ_2, for $[H_4porphine]^{2+}$, + − + − + − + − $[H_4OEP]^{2+}$, $[H_4TPP]^{2+}$, and $[H_4T\text{-}2,6\text{-}Cl_2\ PP]^{2+}$. A map indicating the exact coordinates of the maxima, minima, and saddle points on the strain energy surface for $[H_4porphine]^{2+}$ is given for reference.

counterion strongly affects the conformation of the porphyrin

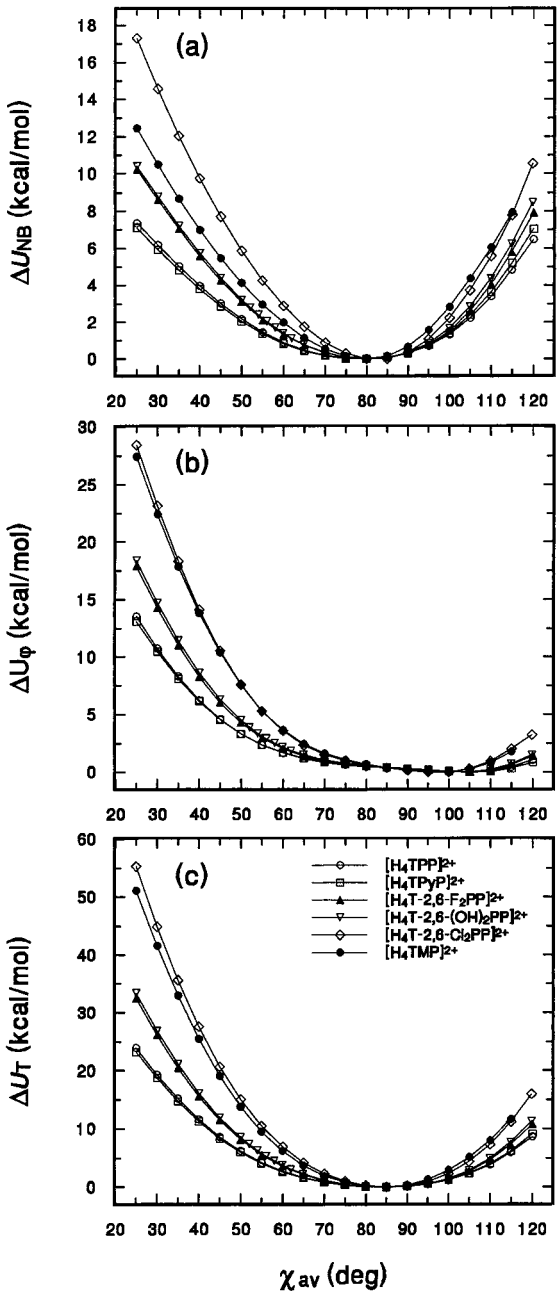

Figure 5. Dependence of the change in van der Waals interaction energy (a), torsional strain energy (b), and total steric energy (c) on the average orientation of the *meso*-aryl groups (χ_{av}) for a series of *meso*-tetraaryl porphyrin diacid derivatives of varying peripheral steric bulk. The optimum orientation of the *meso*-aryl substituents occurs when $\Delta U_T = 0$ kcal/mol.

core. This is believed to be the case in $[H_4OETPP]^{2+}$ and other β-substituted $[H_4TPP]^{2+}$ derivatives.[20d]

All three crystalline forms of $[H_4TPP]^{2+}$ have strongly saddled core conformations and acute porphyrin−phenyl dihedral angles. The porphyrin−aryl group dihedral angles of $[H_4TMP](ClO_4)_2$, on the other hand, are less acute than those of $[H_4TPP](ClO_4)_2$, averaging 63(13)° and 75(15)° in molecules **1** and **2** (Table 1). Consequently, both independent molecules of $[H_4TMP](ClO_4)_2$ show substantially smaller core distortions than $[H_4TPP](ClO_4)_2$, though both are considerably more saddled than $[H_4OEP](ClO_4)_2$. Figure 2 shows that the eight *o*-methyl groups of $[H_4TMP]^{2+}$ are positioned above and below the plane of the porphyrin ring, approximately over the *meso*-carbons. Rotations about the C_m−C_p bonds in response to external effects are therefore likely to be severely restricted. The X-ray data indicate that $[H_4TMP]^{2+}$ is inherently *less flexible* than $[H_4TPP]^{2+}$ and

Table 4. Average Crystallographic Bond Lengths and Bond Angles for Selected Porphyrin Diacids with D_{2d} Core Symmetry[a]

	$[H_4TMTEP]^{2+}$ [b]	$[H_4OEP]^{2+}$	$[H_4TPP]^{2+}$	$[H_4TPyP]^{2+}$ [c]	$[H_4TMP]^{2+}$	$[H_4OBrTPP]^{2+}$ [d]	$[H_4OETPP]^{2+}$ [d]
$N-C_a$	1.379(15)	1.378(6)	1.390(9)	1.386(14)	1.371(7)	1.367(5)	1.370(5)
C_a-C_b	1.438(10)	1.442(4)	1.431(13)	1.445(19)	1.422(5)	1.419(11)	1.448(9)
C_b-C_b	1.378(12)	1.377(4)	1.366(11)	1.326(18)	1.354(6)	1.362(11)	1.373(5)
C_a-C_m	1.386(8)	1.392(6)	1.414(11)	1.396(16)	1.400(6)	1.418(8)	1.407(4)
C_a-N-C_a	109.5(2)	109.4(4)	110.3(10)	109.4(1)	109.6(5)	110.5(1)	110.2(1)
$N-C_a-C_b$	107.5(6)	107.7(4)	106.1(8)	106.4(4)	107.1(2)	106.5(2)	107.1(2)
$N-C_a-C_m$	125.4(8)	125.2(5)	125.9(6)	125.4(7)	126.2(5)	121.3(7)	122.5(4)
$C_a-C_b-C_b$	107.7(5)	107.6(6)	108.7(9)	108.9(8)	108.2(3)	108.2(6)	107.6(4)
$C_a-C_m-C_a$	128.2(10)	127.2(2)	123.2(7)	124.4(9)	124.5(7)	119.8(3)	122.1(4)
$C_m-C_a-C_b$	127.1(7)	127.0(8)	127.9(5)	128.3(13)	126.7(5)	131.9(14)	130.3(5)

[a] Bond distances and bond angles are in Å and deg, respectively. The esd's of the least significant digits are given inparentheses. [b] Reference 20d and f. [c] Reference 20b. [d] Reference 20d.

less susceptible to packing-induced conformational distortions, particularly those caused by rotations of the *meso*-aryl groups. This is consistent with variable-temperature solution NMR studies on $[M(TPP)]^{n+}$ and $[M(TMP)]^{n+}$ derivatives which indicate that free-rotation of the *meso*-aryl groups may be prevented by substitution of the *o*-hydrogens with F or CH_3.[53] Importantly, the lower flexibility of $[H_4TMP]^{2+}$ relative to $[H_4TPP]^{2+}$ is correctly predicted by the present molecular mechanics calculations (Figures 5 and S10).

$[H_4OEP](ClO_4)_2$ (Figure 1) has the least distorted D_{2d} symmetry core conformation of the porphyrin diacids studied, as evidenced by smaller out-of-plane deviations for the pyrrole β-carbons relative to $[H_4TMP](ClO_4)_2$ and $[H_4TPP](ClO_4)_2$ (Figure 3). However, $[H_4TMTEP](ClO_4)_2$,[20d] with only four β-ethyl groups, is less distorted still (Table 3). Increasing the total steric bulk of the β-substituents therefore enhances the intrinsic distortion of the porphyrin core, in consonance with the predictions of our molecular mechanics calculations (Tables 2 and 3). The structure of $-+--------+$ $H_4OEP](TFA)_2$ ($|C_{20}N_4| = 0.30$ Å)[20d] is more distorted than the present structure of $-++++--++$ $[H_4OEP](ClO_4)_2$ ($|C_{20}N_4| = 0.22$ Å, Table 3). Since the difference in ethyl group configuration is not expected to increase $|C_{20}N_4|$ by 0.08 Å, at least by our MM calculations, there may be a genuine counterion effect on porphyrin core conformation in simple β-substituted porphyrin diacids.[54]

The near-constant conformational perturbation introduced by protonating the porphyrin nitrogens should allow the determination of the stereochemical consequences of systematically increasing the distortion of the porphyrin core. Table 4 summarizes the average crystallographic bond lengths and bond angles for β-alkyl and *meso*-tetraaryl porphyrin diacids (D_{2d} symmetry). The average C_a-C_m bond lengths and $C_a-C_m-C_a$ bond angles vary significantly with porphyrin substitution pattern. From the X-ray data given in Tables 2−4, Figure 6a shows that the mean $C_a-C_m-C_a$ angle varies linearly with the magnitude of the D_{2d} -symmetry distortion of the porphyrin core ($|C_b|$). The relationship indicates that much of the strain associated with tipping the pyrrole rings alternately above and below the porphyrin mean plane is taken up at the *meso*-carbons. It is also evident that the average $C_a-C_m-C_a$ angles of the *meso*-substituted derivatives are 2.5−8.5° smaller than those of the β-alkyl derivatives. Part of this difference clearly depends on the extent of porphyrin core distortion.

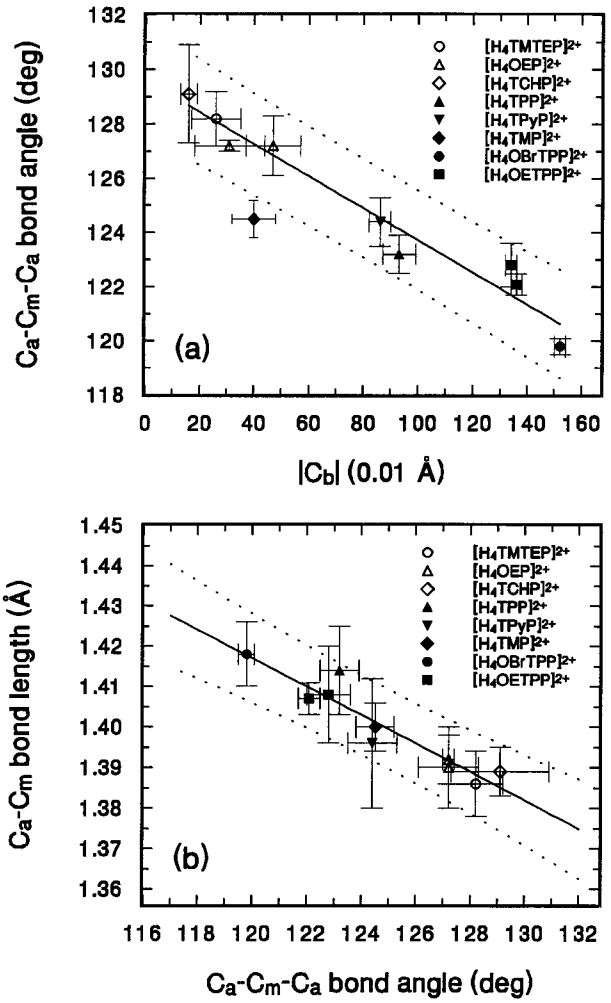

Figure 6. (a) Plot of the relationship between the $C_a-C_m-C_a$ bond angle and the degree of distortion of the porphyrin core (gauged by the parameter $|C_b|$) for a range of peripherally substituted porphyrin diacid derivatives ($R^2 = 0.95$). The dotted line shows the 95% confidence limit; the deviation of $[H_4TMP]^{2+}$ from the trend is discussed in the text. (b) Variation of the C_a-C_m bond length with the $C_a-C_m-C_a$ bond angle for the porphyrin diacids given in part a ($R^2 = 0.87$).

Although the mean $C_a-C_m-C_a$ bond angle correlates with the porphyrin conformation, the fact that $[H_4TMP]^{2+}$ fails to fit the relationship in Figure 6a suggests that the $C_a-C_m-C_a$ angle is determined both by the level of distortion and whether or not the *meso*-carbon is substituted. As noted above, the mesityl groups of $[H_4TMP]^{2+}$ display restricted rotation both

(51) The saddle-point conformations (cols) are slightly lower in energy than the C_{2v} isomer and have C_{2h} symmetry. They differ from the pair of C_{2h} isomers located at $\Psi_1,\Psi_2 = -21°,21°$ and $21°,-21°$, however, by a 90° rotation of the symmetry elements about the porphyrin normal.

(52) A reliable comparison may be made between $[H_4TPP](FeCl_4,Cl)$ ($|C_b| = 1.07$ Å)[20b] and $[H_4OBrTPP](TFA)_2$ ($|C_b| = 1.52$ Å)[20d] to illustrate this point. Both porphyrin diacids show equivalent values of χ_{av} (~36°), where χ_{av} is the mean $C_a-C_m-C_p-C_p$ torsion angle. However, because $[H_4OBrTPP]^{2+}$ (eight β-bromide substituents) is more highly strained than $[H_4TPP]^{2+}$, a larger saddle distortion appears to be necessary to stabilize its structure. (Note that the torsion angle χ may differ from the porphyrin−aryl group dihedral angle measured using the least-squares plane of the porphyrin core and the aryl group. For the purpose of comparison, all *meso*-aryl group orientations listed in Table 2 are values of χ_{av} measured from the coordinates of the X-ray structures or calculated structures.)

(53) (a) Eaton, S. S.; Eaton, G. R. *J. Chem. Soc., Chem. Commun.* **1974**, 576. (b) Eaton, S. S.; Eaton, G. R. *J. Am. Chem. Soc.* **1975**, *97*, 3660.

in solution and in the solid state. This limits the extent to which packing interactions may enhance the saddle distortion of the protonated porphyrin core, accounting for the unexpectedly small value of $|C_b|$ for $[H_4TMP]^{2+}$ and the observed departure of this species from the trend in Figure 6a. If the least-strained $C_a-C_m-C_m$ angle is ~124.6°, as suggested by Hoard,[55] then simple *meso*-tetraaryl derivatives such as $[H_4TPP]^{2+}$, $[H_4TPyP]^{2+}$, and $[H_4TMP]^{2+}$ show minimal angular strain at the C_m positions. β-Substituted porphyrin diacid derivatives, on the other hand, exhibit greater angular strain at the methine carbons (Table 4). A second stereochemical consequence of deforming the porphyrin core, and thus the $C_a-C_m-C_a$ angles, is a concomitant increase in the mean C_a-C_m bond length as the average $C_a-C_m-C_a$ angle decreases (Figure 6b). This stretch−bend relationship mainly reflects the angular dependence of the 1,3-van der Waals interaction between the α-carbons attached to the porphyrin *meso*-carbons.

The conformational surfaces for $[H_4porphine]^{2+}$, $+-+-$ $+-+-$ $[H_4OEP]^{2+}$, $[H_4TPP]^{2+}$, and $[H_4T\text{-}2,6\text{-}Cl_2PP]^{2+}$ (Figure 4) indicate that the D_{2d}-saddled conformation is lower in energy than the C_{2h} conformation. Furthermore, the stability of the D_{2d} isomer increases with increasing substituent bulk, suggesting that a D_{2d}-symmetry distortion of the porphyrin core efficiently minimizes peripheral steric strain. The energy differences between the D_{2d} and C_{2h} isomers of $[H_4porphine]^{2+}$ (~0.8 kcal/mol) and $[H_4OEP]^{2+}$ (~1.0 kcal/mol) are smaller than those calculated for $[H_4TPP]^{2+}$ (1.7 kcal/mol) and $[H_4T\text{-}2,6\text{-}Cl_2PP]^{2+}$ (1.9 kcal/mol). From the geometry of the calculated C_{2h} conformation of $[H_4TPP]^{2+}$ (Figure S9), much of this increase in steric strain in the *meso*-tetraaryl derivatives can be attributed to unfavorable pyrrole−aryl group nonbonded interactions.

Importantly, the calculated inversion barriers ($D_{2d} \rightarrow D_{2d}$) increase with increasing substituent bulk: $[H_4porphine]^{2+}$ (0.45 kcal/mol) < $[H_4OEP]^{2+}$ (0.55 kcal/mol) < $[H_4TPP]^{2+}$ (1.0 kcal/mol) < $[H_4T\text{-}2,6\text{-}Cl_2PP]^{2+}$ (1.9 kcal/mol). This trend parallels that observed in solution by NMR spectroscopy for $[H_4TMTCPP]^{2+}$ (9.2 kcal/mol), $[H_4TETCPP]^{2+}$ (11.7 kcal/mol), and $[H_4TPTCPP]^{2+}$ (11.9 kcal/mol).[14] However, the calculated barriers ($\Delta H^{\ddagger}$) are expected to be lower than the barriers measured in solution ($\Delta G^{\ddagger}$) because, in addition to steric strain, solvation and ion-pairing effects will contribute to $\Delta G^{\ddagger}$.[56] If $\Delta H^{\ddagger}$ is a good arbiter of conformational flexibility, then Figure 4 shows that the peripheral substituents substantially affect *molecular flexibility*. Thus, the strain introduced by increasing the bulk of the peripheral groups has two major effects. First, it favors a D_{2d}-saddled conformation. The degree of distortion, *in the absence of environmental constraints*, therefore increases from $[H_4porphine]^{2+}$ ($|C_b| = 0.34$ Å) to $[H_4T\text{-}2,6\text{-}Cl_2PP]^{2+}$ ($|C_b| = 0.50$ Å, Tables 4 and 5). Second, it leads to an increase in the rigidity of the macrocycle. The barrier to inversion of the D_{2d} conformation therefore increases from $[H_4porphine]^{2+}$ to $[H_4T\text{-}2,6\text{-}Cl_2PP]^{2+}$. A similar conclusion may be reached by considering the relative populations of the D_{2d} and C_{2h} conformational states at 298 K.[57]

A planar conformation with D_{4h} symmetry is not predicted for any of the porphyrin diacids studied on energetic grounds (Table 3). The saddle points connecting the D_{2d} minima on the surfaces shown in Figure 4 (ψ_1, $\psi_2 = 0°$) therefore have C_{2v} rather than D_{4h} symmetry, as shown in Figure S9 for $[H_4TPP]^{2+}$.[60]

The relative flexibilities of several *meso*-tetraaryl porphyrin diacids were determined from the variation of total steric energy with average aryl group orientation (Figure 5). Since the slope of the plot of ΔU_T vs χ_{av} at any point along the reaction coordinate gauges the ease of conformational change at that point, the *molecular flexibility* increases in the order $[H_4TMP]^{2+}$ ≈ $[H_4T\text{-}2,6\text{-}Cl_2PP]^{2+}$ < $[H_4T\text{-}2,6\text{-}F_2PP]^{2+}$ ≈ $[H_4T\text{-}2,6\text{-}(OH)_2PP]^{2+}$ < $[H_4TPP]^{2+}$ ≈ $[H_4TPyP]^{2+}$. (This order prevails for all points along the reaction coordinate.) Figure 5 indicates that nonbonded interactions and torsional strain dominate the energetics of the process. Since torsional strain tends to zero for a planar porphyrin core, the asymmetric variation of ΔU_ϕ with χ_{av} reflects progressive distortion of the porphyrin core as $\chi_{av} \rightarrow 40°$ (Figure S10). Importantly, the prediction that $[H_4TMP]^{2+}$ is *less* flexible than $[H_4TPP]^{2+}$ is consistent with the conclusion based on the barrier to inversion (*vide infra*) and their X-ray structures.

To evaluate the assumption that nonbonded interactions between the pyrrole NH protons drive distortion of the porphyrin macrocycle in porphyrin diacids, we first calculated the energies of the D_{4h}, D_{2d}, and C_{2h} conformations of $[H_4porphine]^{2+}$, followed by the energies of these conformations *less* the strain contribution from the NH protons.[61] From Table 5, the D_{4h} conformation of $[H_4porphine]^{2+}$ lies 2.78 kcal/mol *higher* in energy than the D_{2d} conformation.[62] The data for $[porphine]^{2-}$, however, indicate that in the absence of the pyrrole NH protons, the D_{4h} conformation is 2.70 kcal/mol *more stable* than the D_{2d} symmetry conformation. This is largely due to a higher degree of torsional strain (3.13 kcal/mol) in the latter.

(54) The affinity of $CF_3CO_2^-$ for protonated sapphyrins (Král, V.; Furata, H.; Shreder, K.; Lynch, V.; Sessler, J. L. *J. Am. Chem. Soc.* **1996**, *118*, 1595) and, presumably, porphyrins may be responsible for the unusual crystallographic conformation of $[H_4TCHP](TFA)_2$.[20d] In this species, the $CF_3CO_2^-$ ions bridge *adjacent* NH protons, favoring a stepped core conformation with one pair of cis pyrrole NH groups canted above (and the other below) the porphyrin mean plane (C_{2h}' symmetry). Our calculations show that without the counterions, the stepped C_{2h}' conformation of the X-ray structure refines into a more stable C_{2h} geometry with one pair of trans pyrrole rings lying *in* (and the other pair canted above and below) the porphyrin mean plane. Since a C_{2h} conformation appears to be an accessible local minimum for simple porphyrin diacids (Figure 4), the C_{2h}' conformation of $[H_4TCHP](TFA)_2$[20d] may result from distortion of the C_{2h} conformer by the $CF_3CO_2^-$ ions bridging *cis*-pyrrole NH groups.

(55) Hoard, J. L. *Ann. New York Acad. Sci.* **1973**, *206*, 18.

(56) If the present force field reliably estimates the steric strain contribution to the barrier and the mechanism in solution is the same as that in the gas phase, then comparison of the calculated and observed barriers for $[H_4TMTCPP]^{2+}$ (0.55 vs 9.2 kcal/mol) and $[H_4TETCPP]^{2+}$ (1.4 vs 11.7 kcal/mol) (surfaces not shown) indicates that the solvent contribution to the barrier is large.

(57) There are two and four ways of forming the D_{2d} ($\Delta H_{rel} = 0$ kcal/mol) and C_{2h} ($\Delta H_{rel} = 0.76$ kcal/mol) conformations of $[H_4porphine]^{2+}$, respectively. The statistical contribution to the distribution of the two isomers is given by $\Delta S_{rel} = RT \ln (2/1)$.[58] From the partition function for the system, $N_i = 100 \exp(-\Delta G_i/RT)/\sum_i \exp(-\Delta G_i/RT)$, where N_i is the percentage population of the ith conformation,[59] and the relative stabilities of the D_{2d} ($\Delta G_{rel} = 0.41$ kcal/mol) and C_{2h} ($\Delta G_{rel} = 0.76$ kcal/mol) isomers at 298 K, 64% of a "gas-phase" sample of $[H_4porphine]^{2+}$ should populate the D_{2d} conformation. The percentage population of the D_{2d} conformation at 298 K in the case of $[H_4OEP]^{2+}$ (71%), $[H_4TPP]^{2+}$ (90%), and $[H_4T\text{-}2,6\text{-}Cl_2PP]^{2+}$ (92%) reflects the increase in peripheral steric bulk across the series and the fact that the D_{2d} conformation most effectively minimizes the associated increase in steric strain.

(58) Bond, A. M.; Hambley, T. W.; Snow, M. R. *Inorg. Chem.* **1985**, *24*, 1920.

(59) Comba, P.; Hambley, T. W. *Molecular Modeling of Inorganic Compounds*; VCH: New York, 1995; p 68.

(60) A highly strained conformation in which both pairs of trans pyrrole NH groups become coplanar (D_{4h}) is clearly avoided in the C_{2v} transition state, which has one pair of trans NH groups tipped well below the porphyrin mean plane and a near in-plane location for the second pair.

(61) The D_{4h} conformation of $[H_4porphine]^{2+}$ is inherently unstable and refines into the D_{2d} -saddled conformation in the absence of geometry constraints. However, by using a planar input structure and allowing only the *x*- and *y*-coordinates of the porphyrin core atoms to refine, the total steric energy of the D_{4h} conformation of $[H_4porphine]^{2+}$ can be calculated.

(62) Although there is a 3.34 kcal/mol increase in torsional strain associated with a D_{2d} symmetry conformational distortion, there are significant reductions in the van der Waals energy (ΔU_{NB}, −4.76 kcal/mol), angle-bending energy (ΔU_θ, −1.02 kcal/mol), and bond deformation energy (ΔU_B, −0.41 kcal/mol). These collectively outweigh the unfavorable increase in torsional strain, leading to net stabilization of the D_{2d}-saddled conformation.

Table 5. Strain Energy Components of the D_{4h}, C_{2h}, and D_{2d} Conformations of $[H_4porphine]^{2+}$ and $[Porphine]^{2-}$ [a]

	$[H_4porphine]^{2+}$				$[porphine]^{2-}$ [b]			
	D_{4h}	D_{2d}	C_{2h}	Δ[c]	D_{4h}	D_{2d}	C_{2h}	Δ[c]
U_T[d]	15.211	12.428	13.190	2.783	3.829	6.533	6.663	−2.704
U_b[d]	0.574	0.168	0.228	0.406	0.066	0.068	0.078	−0.002
U_θ[d]	6.179	5.156	5.213	1.023	4.697	4.638	4.631	0.059
U_{SB}[d]	0.088	0.005	0.012	0.083	−0.011	−0.016	−0.018	0.005
$U_{1,4-NB}$[d]	0.721	0.906	0.956	−0.185	1.759	1.647	1.748	0.112
U_{NB}[d]	1.539	−3.221	−2.646	4.760	−3.096	−3.318	−3.296	0.222
U_ϕ[d]	6.000	9.342	9.346	−3.342	0.000	3.134	3.140	−3.134
U_μ[d]	0.110	0.074	0.083	0.036	0.414	0.379	0.380	0.035[a]

[a] All energies are in kcal/mol. [b] Each conformation of $[porphine]^{2-}$ is equivalent to the core geometry of the energy-minimized conformation of $[H_4porphine]^{2+}$ minus the four pyrrole NH protons. The total strain energies of the $[porphine]^{2-}$ conformations give a measure of the intrinsic *core* strain energies of the relevant $[H_4porphine]^{2+}$ conformations. [c] Δ is the energy difference between the D_{4h} and D_{2d} conformations. [d] The components of the total steric energy (U_T) are the bond deformation energy (U_b), angle bending energy (U_θ), stretch-bend energy (U_{SB}), 1,4-van der Waals energy ($U_{1,4-NB}$), through-space van der Waals energy (U_{NB}), torsion angle deformation energy (U_ϕ), and dipole energy (U_μ).

Since protonation of the porphyrin clearly favors a D_{2d}-saddled conformation, the change in total steric energy accompanying the $D_{4h} \rightarrow D_{2d}$ conformational switch can be factored into contributions from distortion of the porphyrin ring and interaction of the NH groups, eq 1

$$\Delta U_T = \Delta U_{NHprotons} + \Delta U_{porphinecore} \quad (1)$$

where $\Delta U_T = -2.78$ kcal/mol and $\Delta\ U_{porphinecore} = 2.70$ kcal/mol (Table 5). The stabilization gained by an out-of-plane configuration for the pyrrole NH groups in the D_{2d} conformation of $[H_4porphine]^{2+}$ is therefore −5.48 kcal/mol. This is the principal driving force behind the conformational switch attending protonation of the free base. Importantly, the calculated increase in core strain energy (2.70 kcal/mol) is in good agreement with that determined by Dirks et al. for $[H_4T\text{-}2\text{-}(OCH_3)PP]^{2+}$ from temperature-dependent ^1H NMR data (2.4 kcal/mol).[63]

Conclusions

The crystal structures of $[H_4OEP](ClO_4)_2$ ($|C_b| = 0.45$ Å), $[H_4TMP](ClO_4)_2$ ($|C_b| = 0.67$ Å), and $[H_4TPP](ClO_4)_2$ ($|C_b| = 0.93$ Å) show that the D_{2d}-symmetry distortion of the porphyrin core depends critically on the nature of the peripheral substituents. The large distortion for $[H_4TPP]^{2+}$ suggests that it is overall more flexible than $[H_4TMP]^{2+}$. This conclusion is supported by molecular mechanics calculations which indicate that the strain energy penalty to rotation of the *meso*-aryl groups (and concomitant distortion of the porphyrin macrocycle) increases in the order $[H_4TPyP]^{2+} < [H_4TPP]^{2+} < [H_4T\text{-}2,6\text{-}(OH)_2\ PP]^{2+} \approx [H_4T\text{-}2,6\text{-}F_2PP]^{2+} < [H_4T\text{-}2,6\text{-}Cl_2PP]^{2+} \approx [H_4TMP]^{2+}$. The calculated (*in vacuo*) barrier to conformational inversion also increases with increasing substituent bulk, $[H_4porphine]^{2+} < [H_4OEP]^{2+} < [H_4TPP]^{2+} < [H_4T\text{-}2,6\text{-}Cl_2PP]^{2+}$, suggesting that steric crowding decreases molecular flexibility. Since $[H_4OEP]^{2+}$ is calculated to be modestly less distorted than $[H_4TPP]^{2+}$, but is in fact considerably less distorted (less flexible) in the solid state, our results suggest that differences in conformation between analogous $[M(OEP)]^{n+}$ and $[M(TPP)]^{n+}$ derivatives (the latter are always more distorted) are largely, though not entirely, the result of environmental effects on the molecular conformation.

Acknowledgment. We thank the National Institutes of Health for support of this research under Grant GM-38401 (W.R.S). Funds for the purchase of the FAST area detector diffractometer were provided through NIH Grant RR-06709. H.M.M. thanks the University of the Witwatersrand, through the Centre for Molecular Design, and the Foundation for Research Development, Pretoria, for financial support.

Supporting Information Available: Complete crystallographic details, atomic coordinates, anisotropic thermal parameters, fixed hydrogen atom coordinates, bond lengths, and bond angles for $[H_4OEP](ClO_4)_2$, $[H_4TPP](ClO_4)_2$, and $[H_4TMP](ClO_4)_2$ (Tables S1−S18). Comparison of X-ray and MM-calculated bond lengths, bond angles, and torsion angles for eight porphyrin diacids (Tables S19−S42) and listing of new force field parameters (Table S43). Diagrams showing the perpendicular displacements of the porphyrin core atoms from the nitrogen-atom mean planes of $[H_4OEP](ClO_4)_2$, $[H_4TPP](ClO_4)_2$, $[H_4TMP](ClO_4)_2$ (molecule **1**), and $[H_4TMP](ClO_4)_2$ (molecule **2**) (Figures S1−S4); ORTEP diagrams of $[H_4TPP](ClO_4)_2$ and $[H_4TMP](ClO_4)_2$ (molecule **2**) (Figures S6 and S7). Diagram of MM2 force field atom types (Figure S5). Fits of MM-calculated and X-ray structures (Figure S8), selected conformations of $[H_4TPP]^{2+}$ from Figure 4 (Figure S9), variation of tetraaryl porphyrin diacid β-carbon displacements (Figure S10) and $[H_4TMP]^{2+}$ conformations (Figure S11) with χ_{av} (68 pages.) See any current masthead page for ordering and Internet access instructions.

JA9716214

(63) Dirks, J. W.; Underwood, G.; Matheson, J. C.; Gust, D. *J. Org. Chem.* **1979**, *44*, 2551.